Journal Pre-proofs

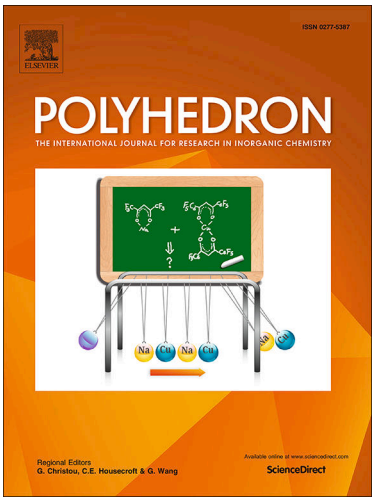

Gold(I), Silver(I) and Copper(I) Complexes of 2,4,6-trimethylphenyl-3-benzoylthiourea; Synthesis and biological applications

Umar Ali Khan, Amin Badshah, Muhammad Nawaz Tahir, Ezzat Khan

PII: S0277-5387(20)30142-X
DOI: https://doi.org/10.1016/j.poly.2020.114485
Reference: POLY 114485

To appear in: *Polyhedron*

Received Date: 31 January 2020
Revised Date: 27 February 2020
Accepted Date: 28 February 2020

Please cite this article as: U. Ali Khan, A. Badshah, M. Nawaz Tahir, E. Khan, Gold(I), Silver(I) and Copper(I) Complexes of 2,4,6-trimethylphenyl-3-benzoylthiourea; Synthesis and biological applications, *Polyhedron* (2020), doi: https://doi.org/10.1016/j.poly.2020.114485

Gold(I), Silver(I) and Copper(I) Complexes of 2,4,6-trimethylphenyl-3-benzoylthiourea; Synthesis and biological applications

Umar Ali Khan[1], Amin Badshah[2], Muhammad Nawaz Tahir[3], Ezzat Khan[1*]

[1]Depatrment of Chemistry, University of Malakand, 18800 Chakdara, Khyber Pakhtunkhwa, Pakistan

[2]Department of Chemistry, Quaid-i-Azam University, Islamabad, Pakistan

[3]Department of Physics, University of Sargodha, 40100 Sargodha, Punjab, Pakistan.

[*]Corresponding Author: ekhan@uom.edu.pk

Abstract

2,4,6-trimethylphenyl-3-benzoylthiourea **(L)** and its gold(I), silver(I) and copper(I) complexes were synthesized. Treatment of **L** with $HAuCl_4$, $AgNO_3$ and CuI in CH_3CN afforded complexes of general representation, M(L)X**,** where M/X = Au/Cl (**1**), Ag/NO_3 (**2**), Cu/I (**3**). Reaction with Au^{3+} salt afforded two products, wherein complex containing Au^{+} (reduced under normal and aerobic reaction conditions ca. 66% on NMR time scale) was confirmed by x-ray diffraction for a single crystal of complex **1**. The minor fraction (ca. 33%, from ^{1}H-NMR data) in the reaction mixture was identified as complex **4** with a general formula $[AuL_2]Cl_3$. Reaction with $AgNO_3$ and CuI exclusively afforded pure products **2** and **3**. Ligand **L** and complexes **1-4** were characterized by UV/visible, FT-IR and ^{1}H-, ^{13}C-NMR spectroscopy. Complex **1** is crystalline in nature and good quality crystals were obtained which allowed for collection of diffraction data and the structure was thus confirmed. Solution state and solid state structures have been compared. The resultant complexes were tested for their cytotoxicity, antibacterial, antifungal, antioxidant and DNA binding activities. Complex **1** (Au based) showed promising activities in comparison with the available selected drugs used as standards.

Keywords: 2,4,6-trimethylphenyl-3-benzoylthiourea; M(I) complexes; Characterization; X-ray structure; DNA binding.

1. Introduction

Transition metals have tremendous role in the development of new metal based drugs to combat several human ailments. Transition metal complexes exist both in anionic and neutral forms. Metal ion is normally surrounded by ligands which determine the reactivity in a desired direction and many of metal complexes are in field to fight against several human related diseases like carcinomas, lymphomas, diabetes, neurological disorder and anti-inflammatory disease.[1, 2] Transition metal complexes exist in a variety of oxidation states and this characteristic enable them to accommodate a variety of organic molecules or ligands around them. The incorporation of different ligands can tune the properties of metal ions in a desired manner thus making metal based drugs promising pharmacological candidates. A number of metal complexes are in field which encourage studies for exploration of new metallodrugs with attractive properties like biological potency, easy accessibility, least toxicity and improved physical profile. Among transition metals gold, silver, copper, nickel and zinc have been in use for their non-biological and biological applications[3, 4].

The pharmacological applications of metal complexes depend upon the type of metal, its oxidation state and nature of ligand(s). Different metal ions with same ligands and same metal with different ligands exhibit far different biological properties. Currently a number of metal based drugs have been investigated showing promising *in vitro* results, but during *in vivo* studies they suffer from some limitations and very less are recommended for clinical trial. The challenge for a metallodurg is its *in vivo* stability and compatibility with biological system which entirely depends on the selection of an adequate ligand and its counter metal ion[5, 6]. Among ligands thiourea derivatives enriched with O and N donors in addition to its S functionality, have attracted much interest because of their diverse and strong coordination ability, variety of coordination modes, biocompatibility, accessibility and ease of modification. Thiourea derivatives exist both in neutral

(S donor only) and anionic (N donor, N, S donor, N, S, O donor) state[7]. To date, a number of metal complexes of thiourea derivatives especially those containing Cu, Ag and Au as central metal ions have been investigated with excellent biological applications like DNA binding, antimicrobial, cytotoxic, anti-arthritic, and antioxidant agents[8-10].

In continuation to our previous work [11] on thiourea ligands and their complexes with a variety of metal ions, here we report synthesis and complexation of 2,4,6-trimethylphenyl-3-benzoylthiourea ligand with Au(I), Ag(I), Cu(I) and Au(III) metal ions. Structure of complex **1**, was determined with the help of X-ray diffraction and experimental data were calculated and compared. The ligands and its complexes were tested for their preliminary biological evaluation of DNA binding, cytotoxicity, free radical scavenging and antibacterial potency. Activities of all complexes are promising as compared to corresponding standard drug.

2. Experimental

2.1 General

All chemical reagents and metal salts were purchased from Sigma Aldrich and Merck and were used without further treatment to purify them. All organic solvents were distilled prior to use. The NMR spectra were recorded on BRUKER AVANCE 300 MHz spectrometer in deuterated solvents as mentioned against each compound. The FT-IR spectra were recorded with Shimadzu 8300 spectrometer as KBr discs in the frequency range of 4000-200 cm^{-1}. The UV spectra were recorded using Shimadzu UVPC-1800 UV-visible scanning spectrometer (sample path length 1.0 cm) in the range of 800-200 nm.

2.2 **Synthesis of 2,4,6-trimethylphenyl-3-benzoylthiourea, L**

Ligand L was prepared by following the literature procedure[12]. The white precipitates obtained were recrystallized in ethanol/chloroform mixture (1:1 v/v). Yield, 78%; m.p = 154-

156°C; ^{1}H-NMR (Acetone-D_6); δ (ppm) = 11.80 (br, 1H, NH), 10.20 (br, 1H, NH), 7.99-7.96 (m, 2H, Ar-H), 7.57-7.38 (m, 3H, Ar-H), 6.80 (s, 2H, Ar-H), 2.72 (s, 3H, CH_3), 1.92 (s, 6H, $2CH_3$); ^{13}C-NMR (Acetone-D_6); δ (ppm) = 181.1, 168.2, 137.5, 136.0, 135.4, 134.1, 133.6, 132.7, 130.0, 127.8, 20.5, 17.6; FT-IR ν(cm^{-1}) = 3245w, 3156w, 2917w, 1689m, 1500s, 1475s, 1209m, 1139s, 699s, 653s, 514m.

2.3 Synthesis of 2,4,6-trimethylphenyl-3-benzoylthiourag*old(I) chloride, 1*

A solution containing L (100 mg, 0.33 mmol, in 15 mL acetonitrile) was added drop wise to a solution of $HAuCl_4$ (113 mg, 0.33 mmol), in the same solvent (15 mL). The reaction mixture was allowed to stir overnight at room temperature, during this time the pale yellow color of the solution mixture turned colorless. The solution was filtered, solvent and other readily volatile materials were evaporated under reduced pressure and NMR was measured in acetone-D_6, which indicated two products in a ratio 66% (**1**) and 33% (**4**). A portion of solid was dissolved in acetonitrile and the resulting solution was allowed to evaporate slowly. After few days colorless needle like crystals appeared, they were separated from the mother liquor and a suitable crystal was selected for single crystal analysis, confirming complex **1**, the major fraction in the mixture.

Complex **1**: ^{1}H-NMR (Acetone-D_6) δ (ppm) = 10.09 (br, NH), 9.85 (br, NH), 8.18-8.10, 7.73-7.64, 7.61-7.56 (m, m, m, CH, Ar), 2.34 (s, Me), 2.33 (s, Me); FT-IR ν(cm^{-1}) = 3210w(br), 3130w(br), 2916w(br), 1658m(br), 1498s(br), 1259m(br), 1146s(br), 686s(br).

2.4 Synthesis of Complex 2,4,6-trimethylphenyl-3-benzoylthiourea silver(I) nitrate, **2**

Ligand (100 mg, 0.33 mmol) was treated with $AgNO_3$ (56.5 mg, 0.33 mmol) in acetonitrile in the same way as stated for complex **1** above. During the course of overnight stirring, a color change from pale yellow to colorless was observed, which indicated reaction completion. Solid unreacted salt material were separated through filtration and the resultant solution was kept for

slow evaporation. After few days solid powder of the proposed compound were obtained and were accordingly analyzed. Yield = 70%; m. p = 290-300°C; ^{1}H-NMR (Acetone-D_6) δ (ppm) = 10.10 (br, 1H, NH), 9.88 (br, 1H, NH), 8.18-8.15, 7.73-7.67, 7.61-7.52 (m, m, m, 5H, Ph), 6.94 (s, 2H, CH), 3.03 (s, 3H, Me), 2.27 (s, 6H, 2Me); FT-IR ν(cm^{-1}) = 3244w, 3128w, 2917w, 1688s, 1523s, 1500s, 1474s, 1288m, 1209s, 710s, 515m.

2.5 Synthesis of 2,4,6-trimethylphenyl-3-benzoylthioureacopper(I) iodide, **3**

CuI (63 mg, 0.33mmol) and ligand (100 mg, 0.33 mmol) were mixed together in 15 mL acetonitrile and the reaction was proceeded in the same way as stated for compounds **1** and **2**. After 2h, white precipitate were obtained, were filtered off, washed with ether and dried in open air. Crystallization in various solvents did not lead to the formation of crystallographically suitable crystals. Yield = 68%; ^{1}H-NMR ($CDCl_3$) δ (ppm) = 12.11 (br, 1H, NH), 10.37 (br, 1H, NH), 7.99-7.92, 7.62-7.47 (overlapped multiplet, 5H, Ph), 6.96 (s, 2H, CH), 2.32 (br, 3H, Me), 1.36 (s, 6H, Me); FT-IR, ν(cm^{-1}) = 3270br, 2916w, 2851w, 1673m, 1639m, 1504s, 1486s, 1258m, 709m, 655s, 435m.

2.6. Synthesis of bis(2,4,6-trimethylphenyl-3-benzoylthiourea)gold(III) chloride, **4**

Complex **4** was obtained as block crystals together with needles of complex **1** and the crystals were separated under microscope. UV/Visible, $CHCl_3$ solution, λ_{max}(nm)/ε(M^{-1}cm^{-1}): 303/15228. ^{1}H-NMR (Acetone-D_6) δ (ppm) = 12.40 (br, 1H, NH), 10.98 (br, 1H, NH), 8.10 (m, CH, Ar), 7.79 (m, CH, Ar), 7.65 (m, CH, Ar), 7.03 (s, 2H, Ar), 2.87 (s, 3H, CH_3), 2.29 (s, 6H, 2CH_3); FT-IR, ν(cm^{-1}) = 3303m, 3131w, 3015w, 2915w, 1679s, 1556s, 1508s, 1485s, 1236s, 1171m, 1066m, 832m, 585m.

3. X-ray crystallography

The X-ray diffraction data of complex **1**, were collected with the help of Bruker kappa APEXII CCDC diffractometer (Chemical formula $C_{17}H_{18}AuN_2ClOS$, M_r 530.81, crystal system monoclinic, space group $P2_1/c$, temperature 296, a 8.059(7) Å, b 14.254(13) Å, c 15.795(15) Å, β 102.22°, volume 1773.3(3) $Å^3$, Z 4, radiation type Mo-Kα, μ 8.57 mm^{-1}, crystal size 0.38×0.34×0.30 mm, absorption correction multi-scan, T_{min} 0.160, T_{max} 0.215, number of measured reflections 11252, independent reflections 3842, observed reflections with [$I > 2\sigma(I)$] 3201, R_{int} 0.042, R[$F^2 > 2\sigma(F^2)$] 0.027, w$R(F^2)$ 0.067, S 1.02 and number of parameter 211). Structure solution and refinements were accomplished by taking advantage of software PLATON, WinGx, SHELXL and SAINT[13-16].

3.1 Theoretical Studies

The complex 1 was investigated by DFT using B3LYP method and LANLD2Z basis set [17-19], while the ligand **L** by the same method but 6-31G basis set was used instead, employing Gaussian view 09 package with the support of Gaussian view visualization program [20]. Optimized geometrical parameters such as bond angles and lengths, for ligand **L** and complex **1** have been calculated[21]. The highest occupied molecular orbitals (HOMO) and Lowest Unoccupied molecular orbitals (LUMO) and electrostatic potentials of the complex were also analyzed[18]. Global reactivity parameters such as electronegativity (A), ionization potential (I), hardness (η), softness (σ) electronegativity (X), chemical potential (μ) and electrophilicity (ω) by using the following equations[22].

4. Cytotoxicity Studies

4.1 Brine shrimp lethality bioassay

The selected compounds were screened for bioactivity using shrimp lethality test to check the cytotoxic activity of ligand and its complexes **1-3**. Lethality test was performed in a 96 well plate against brine shrimp (*Artemia salina*) larvae as previously described at 30-32°C in simulated seawater (38 g/L supplemented with 6 mg/L dried yeast) in a specially designed two-compartment plastic tray.[23] The assay system was performed by taking 10 bijoux bottles for different concentrations of test compounds. A 100 mg of each test compound (ligand and respective complexes, each) were weighed and dissolved in mixture of solvents containing 1 mL DMSO and 2 mL of seawater. Two-fold dilution was carried out to prepare a series of concentrations ranging from 100 to 0.195 mg/mL. Afterwards, 10 mature phototropic nauplii were harvested with the help of Pasteur pipette and transferred to each bijoux bottle using magnifying glass for correct counting of nauplii. Positive and negative control wells included serial concentrations of doxorubicin and 1% DMSO, respectively. The setup was allowed to stay for 24 h at normal conditions of temperature. After 6 and 24 h the bottles were observed using magnifying glass and the number of survived larvae were counted and recorded. Percent of mortality of nauplii was calculated for each concentration of the respective sample. The median lethal concentration (LC_{50}) was determined by plotting graph of mean percent mortality versus log of concentration. The LC_{50} value greater than 1.0 mg/mL, suggests that the compound is nontoxic. Percent mortality can be calculate by using the following formula [24, 25].

$$\% \text{ Mortality} = \frac{N0 - Ni}{No} \times 100$$

(Where, N_0 = number of nauplii taken, N_i = number of napulii dead)

5. Antibacterial activity

Susceptibility of extracts against bacterial species was tested according to formerly described procedure[26]. Three Gram negative strains (*Bordetella bronchiseptica*, *Salmonella typhimurium* and *Klebsiella aerogenes* also known as *Enterobacter aerogenes*, ATCC # 4617, 14028 and 13048, respectively) were selected during this study. The strains were cultured in nutrient broth media and incubated for 24 h at 37°C. Sterilized deionized water was used to adjust the turbidity to 10^4 CFU/mL by comparing with McFarland 0.5 $BaSO_4$ turbidity standards. The refreshed inoculum (100 µL) was then swabbed onto Petri plates containing 20 mL nutrient agar. Test samples (5 µL of 20 mg/mL DMSO; 100µg/disc) were infused on sterile filter paper discs (6 mm) and placed on seeded nutrient agar plate. Cefixime-USP at a concentration of 20 µg/disc and DMSO impregnated discs were included as positive and negative controls, respectively in order to assess the activity in a better way. After 24 h incubation, clear zones of growth inhibition were measured manually. The following formula was used to calculate the percent bacterial inhibition.

$$\% \text{ Inhibition} = \frac{A}{B} \times 100$$

(A = linear growth (mm) in test sample and B = linear growth (mm) in control)

6. Antifungal activity

Antifungal activity of compounds **1-3** and **L** was evaluated by following the described standard protocol[26]. The fungal strains (*Aspergillus fumigatus*, *Fusarium solani and Mucor* specie, commercially available under FCBP # 66, 0291 and 0300, respectively) were purchased from fungal culture bank of Pakistan, they were accordingly cultured on SDA. Prior to the sensitivity determination, the spores were harvested in 0.02% Tween 20 solution and turbidity was adjusted according to McFarland 0.5 turbidity standard. A 100 µL sample of each harvested spores was swabbed on plates containing 25 mL sterilized SDA. Filter paper discs loaded with 5 µL of

test sample (20 mg/mL DMSO; 100 µg/disc) as well as standard available antifungal terbinafine (50 µg/disc) and DMSO were placed on seeded SDA plates. The plates were incubated at 28°C for 24-48 h. Thereafter, clear zones of inhibition around discs were observed and measured using Vernier caliper.

7. Antioxidant assay

Free radical scavenging activity of complexes **1-3** was determined by previously reported methods against a robust radical, 2,2-diphenyl-1-picrylhydrazyl (DPPH)[27]. The scavenging or reducing activities of metal complexes due to hydrogen atom or electron donation were measured by color change of DPPH from purple to pale yellow. Absorbance of free DPPH solution (50 mM DMSO) was measured at 517 nm represented by $A_{(blank)}$ in the following equation. The DPPH (1.0 mL) was added to each sample solution of complexes and the resultant mixtures were incubated for 30 min in dark, at ambient temperature (23±1°C). The absorbance of each solution was measured (represented by A_{sample} in the equation given below) and percent scavenging activity was calculated as below.

$$\text{Percent Inhibition} = (A_{balnk} - A_{sample}/A_{blank}) \times 100$$

The IC_{50} of each sample was determined by plotting %I vs concentration. All measurements were carried out in triplicate and their mean was considered for calculations [28-31].

8. DNA Binding studies

8.1 Spectrophotometric method

The binding activities of complexes **1-4** with CT-DNA were measured in 5 mM Tris-HCl buffer at pH 7.2. Stock solution of DNA in double distilled water was prepared and stored at 4±1°C. The absorbance of solution containing DNA was measured at 260 and 280 nm, the ratio

1.9 indicates that the DNA is sufficiently free from protein. The concentration of the stock solution was determined by measuring absorption at 260 nm using its molar absorption coefficient (ε_{260} = 6600 $M^{-1}cm^{-1}$). The absorption titration was performed for solutions of 100 μM of each complex in the presence of various concentrations of DNA (0.001 μM - 0.032 μM). The spectra were recorded after the addition of equal amounts of different concentrations of DNA to different solutions of complex **1-4** of same concentration followed by equilibration for 10 min. The intrinsic binding constant, K_b was calculated as per equation below [32, 33].

$$[DNA]/[\varepsilon_a-\varepsilon_f] = [DNA]/[\varepsilon_b- \varepsilon_f] + 1/K_b [\varepsilon_b- \varepsilon_f]$$

Where, [DNA] = concentration of DNA, ε_a = the extinction coefficient for the absorption band at the given DNA concentration and ε_f, ε_b = the extrinsic coefficients of free metal complex and of the complex fully bounded to DNA. A plot of $[DNA]/[\varepsilon_a- \varepsilon_f]$ vs [DNA] gives a slop $1/[\varepsilon_a- \varepsilon_f]$ and intercept Y equal to $1/K_b [\varepsilon_b- \varepsilon_f]$. The binding constant is regarded as the ratio of the slop to intercept.

8.2 Viscosity measurements

Viscometric titration was carried out using ubbelodhe viscometer maintained at 25°C immersed in water bath. The concentration of DNA was kept constant and concentration of the tested complexes was increased gradually. Different concentration of the respective complex was introduced into DNA solution present in viscometer and equilibrated for some time. Flow time was measured with stop watch. Each experiment was performed in triplicate and average flow time was calculated. Relative viscosity of DNA in the presence and absence of complex was determined using the following relation.

$$\eta'_{sp}/\eta_{sp} = \{(t_{complex}-t_0)/t_0\}/\{(t_{control}-t_0)t_0\}$$

where, η'_{sp} and η_{sp} are the specific viscosity of DNA-Compound complex and DNA, respectively; $t_{complex}$, $t_{control}$ and t_0 are the flow time of DNA-compound complex, pure DNA and buffer, respectively. Data were presented as $(\eta/\eta_o)^{1/3}$ versus [complex]/[DNA] where, η is the viscosity of DNA with complex and η_o is the viscosity of free DNA.[33, 34]

9. Result and Discussion

9.1 General considerations

Thiourea derivative **L** and its Complexes **1-4** were characterized by UV-visible, FT-IR, NMR spectroscopy and structure of complex **1** was confirmed by x-ray diffraction for a single crystal. The UV-visible spectra of the free ligand and the respective complexes provided enough information regarding product formation. An absorption peak at 243 nm with a broad shoulder at 282 nm was observed for the free ligand (Figure S1). The shoulder at 282 nm may be predominantly assigned to C=S, π-π* transition. In complexes the shoulder disappeared, thus revealing the stabilization of π-electron as a result of electron flow towards metal ion. The observation also supports the coordination through S atom[6]. The UV/Visible spectrum of complex **4** is different from other three complexes. The shoulder peak at higher wavelength was nor resolved however, the deformed structure of the parent peak indicate additional electronic excitations such as M-X in complexes **1-3**. The absence of shoulder peak in the UV spectrum of complex **4**, indicates that the molecule is lacking of M-X moiety as has been reported for Au(III) complexes [35]. Molar absorptivity, calculated from the same data was also very close to the data for structurally analogous compounds.

The FT-IR spectra of ligand **L** give a typically broad peak at 3245, 3156 cm^{-1}, corresponds to stretching frequency of N-H bonds, 2917 cm^{-1} for C-H, a strong peak at 1689 cm^{-1} for C=O and at 1209 cm^{-1} for C=S bond. In complexes **1**, the existence of peak around 1658 cm^{-1} typically broad

indicates traces of compound **4**, due to which the peaks corresponding to C=O do not resolve. Further a shift to lower wave number supports coordination of ligand with the metal ion. The signal corresponds to the same functional group appear at 1688 and 1673 cm^{-1} in complex **2** and **3,** respectively. Slight change in wave number of C=O group (1688 in comparison to 1689 cm^{-1} of the free ligand) in compound **2** rules out the involvement of this group in coordination, and it can be clarified that the ligand is monodentate S-donor. Further shift of the peak 1673 cm^{-1} indicates that the ligand predominantly affords a chelate through S and O atoms, affording three coordinated complex, **3**. In complex **4**, the C=O bond stretching appear at 1679 cm^{-1} which is in close agreement with bidentate (S,O-donor) behavior of the ligand. Other peaks in IR spectra of compounds agree well with the proposed structure as given in *Scheme 1*. The C=S bonds in complexes 1-4, show negative shift indicating coordination of ligands with metal ion *via* C=S site. The NMR spectroscopy is a reliable technique which provides enough information regarding the proposed structure of the ligand, **L** and its complexes. Characteristic broad signals at 11.80 and 10.20 ppm can be assigned qualitatively to two protons bonded to N atoms. A sharp singlet in the aromatic region and two sharp signals in aliphatic region can be assigned unambiguously to CH and Me protons of the 2,4,6-trimethylphenyl group of the unsymmetrical thiourea. Similarly ^{13}C-NMR spectra contains signals at 181.1 and 168.2 ppm, correspond to CS and CO carbons, respectively. Two signals in aliphatic region with relative intensities of 1:2, clearly indicate the presence of chemically different Me groups. The ^{1}H–NMR signals of complexes in characteristic regions provide enough information regarding formation of the proposed complexes. These data of gold complex reveal formation of two products where chemical shifts of NH groups of the ligand and CH and Me groups of 2,4,6-trimethylpheny moiety are quite helpful in proposing structure of these complexes. Structure of minor (ca. 33%) fraction can be proposed as compound **4**, shown in Scheme 1, which is crystalline in nature and can easily be separated under microscope

from the major (66%) unexpected product, complex **1**. The NMR spectrum of compound **2** with signals at 10.10 and 9.88 ppm, indicate formation of a single product and the same can be supported by the appearance of aromatic CH protons (at 6.94 ppm) of 2,4,6-trimethylphenyl group. The same signals for compound **3** were observed at 12.10 and 10.37 ppm for NH groups and at 6.96 ppm for CH of 2,4,6-trimethylphenyl group. From a consistent IR and NMR data sets it can be concluded that Cu is predominately three coordinated with trigonal planar geometry as shown in Scheme 1. The chemical shift values of compound **1**, **2** and **3**, **4** are in support of monodentate and bidentate nature of the ligand, respectively. The presence of two NH signals in NMR spectra of ligand and complexes confirm that no coordination through N-atom has occurred. [36, 37]

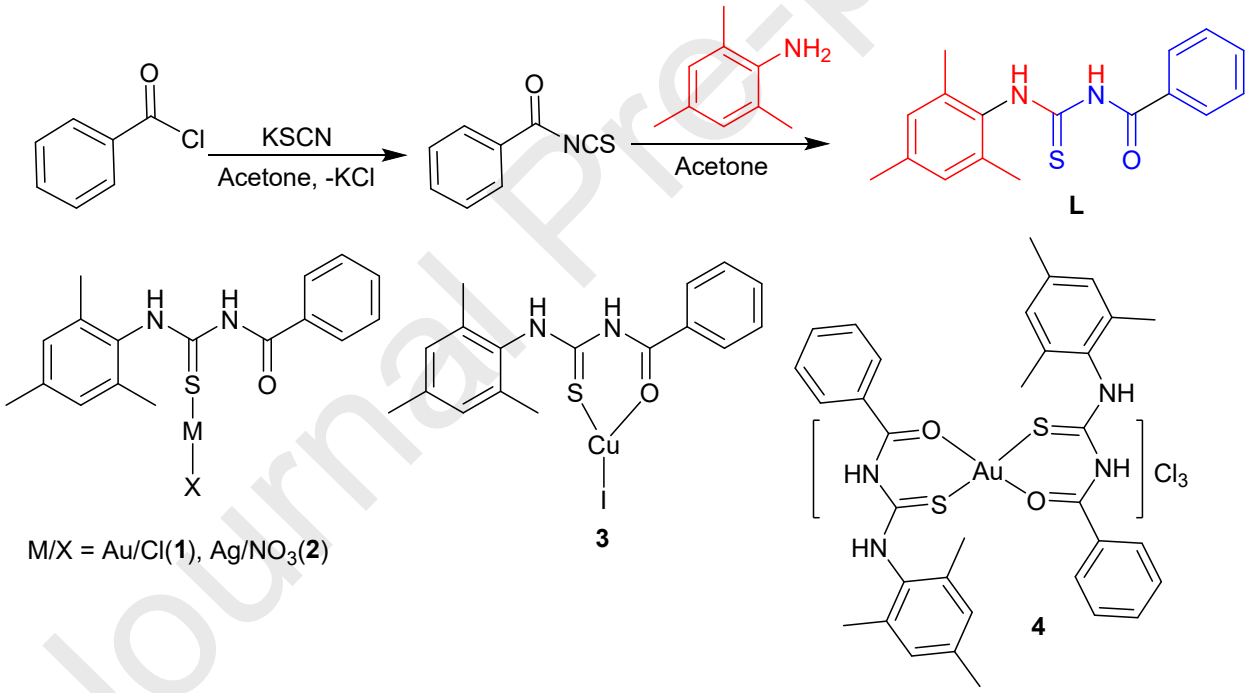

Scheme 1 Synthesis of ligand, **L** and proposed structures of its complexes, **1-4**.

9.2 Single Crystal Analysis and comparison of experimental and theoretical parameters of complex 1

Complex **1** was isolated from the mixture as colorless needles and structure for a single crystal with suitable dimensions was determined as shown in **Figure 1**. The compound crystalizes

as monoclinic system with space group P21/c, a=8.0593(7) (Å), b=14.2537(13) (Å), c=15.7948(15) (Å), β=102.224(4). The reaction was carried out in CH_3CN in open air therefore reduction of Au ion from +3 to +1 was observed wherein the major component of the mixture was found to be a linear complex, **1** [37]. The metal ion in complex **1** accommodates the ligand through it S site and O remains uncoordinated. The Au-S and Au-Cl bond lengths are 2.265 and 2.252 Å, respectively. The Au-S bond with considerably shorter distance as compared with other homoleptic thiourea complexes [38, 39] is predominantly because of the presence of chloro function in *trans* position, across metal ion. This observation also clarifies the nature of M-Cl bond being expected to be labile in further relevant studies. The Cl-Au-S fragment is considerably bent with a bond angle of 174.87°. A close view of intermolecular interactions of non-covalent nature did not give any clue to explain the deviation from linearity as we have reported recently for a Ag complex, where the geometry around metal ion was pseudo-five coordinated.[40] The inter-/intramolecular non-covalent interactions can be found in molecules of compound **1**, wherein no aurophilic interactions were detected. The most important interaction is Cl···C=O with a separation distance between Cl···C 3.410 Å and the same function also interacts with C4H with a separation distance of 3.626 Å. The N2···O1 within the same molecule interacts with each other through intramolecular H-bonding (2.626 Å). This interaction inhibits the ligand up to some extent to act as bidentate and also the donor sites S and O are stabilized in a *trans* manner with respect to each other at 168.67°. Other interactions were also found due to which the supramolecular structure extends in a 2D fashion, a representative dimmer unit is shown in **Figure 2** with selected interactions. Similarly, the compound is also lacking agostic interactions as has been reported for linear Au-thiourea complexes.[41]

Geometry optimization of ligand **L** and the respective complex **1** was carried out with the intent to correlate solid state (experimental) and gas phase structure (optimized). The optimized

structures with complete atom labelling and numbering scheme, of **L** and complex **1** are shown in Figure S2 and S3, respectively. The calculated structural parameters (bond lengths and angles) are summarized together with experimental data in *Table 1*. Considering bond lengths, the identical value was found to be 1.480 Å for (C1-C7). The least deviated value was found to be 0.0087 Å for (N2-C9) and the most deviated values was found for Au1-S1 with 0.2005 Å. In case of bond angles the identical value was found for N1-C8-S1 to be 119.9°. The least deviation was observed for theoretical and experimental value of C2-C3-C4 with a difference of 0.18° and the most deviated angle was Cl1-Au1-S1 (2.59°). Critical overview of the calculated and experimental data are in close agreement with each other.

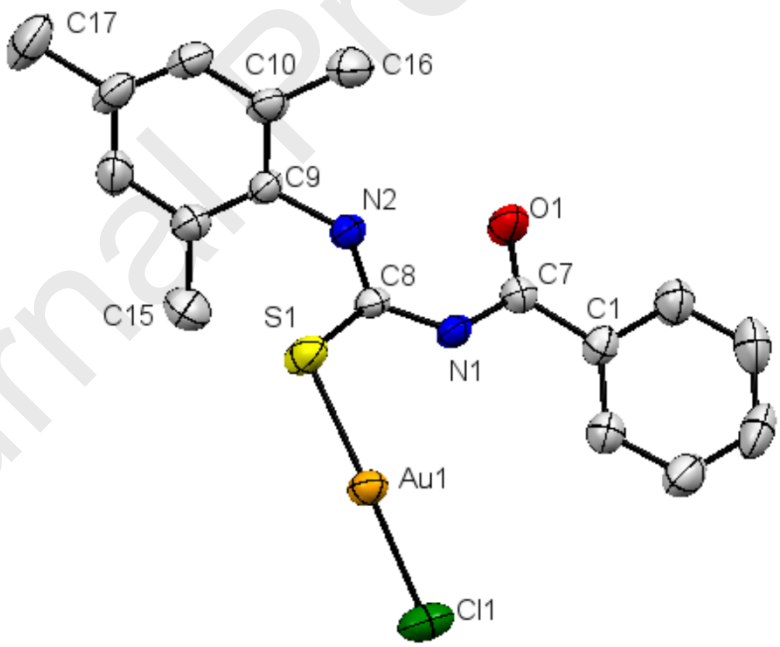

Figure 1 Solid state structure of Complex **1**, with 50% thermal ellipsoids, partial numbering scheme, all hydrogen atoms are omitted for clarity.

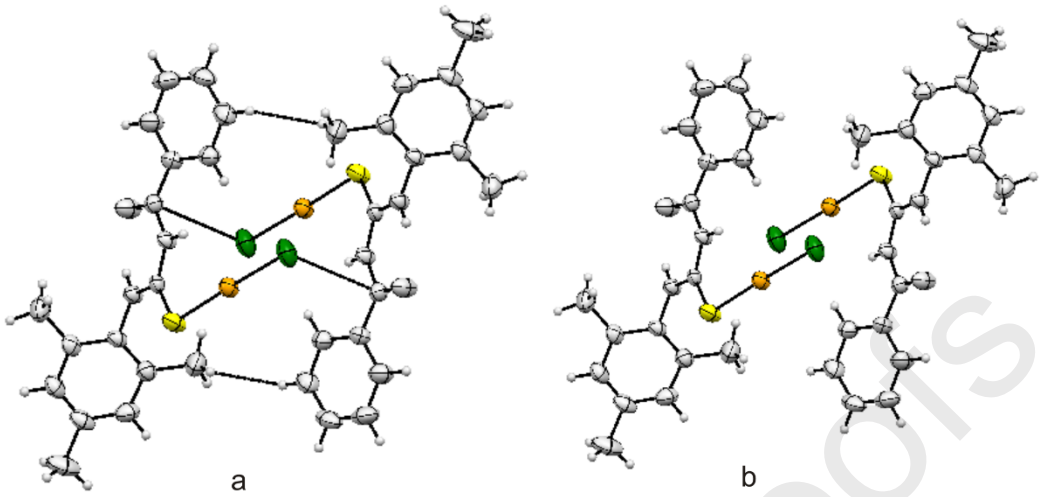

Figure 2 Extended structure of complex **1,** (a) short contacts wherein Cl function and carbonyl carbon (C=O) are involved, Hydrogen atoms of methyl belong to 2,4,6-trimethylphenyl and CH of phenyl moiety are also linked. Hanging contacts which extend the structure further are deleted for clarity reasons. (b) Same view of molecules without short contacts.

Table 1 Summarized bond lengths (Å) and angles (°) obtained experimentally and theoretical Calculations using B3LYP/LANLD2Z

	Bond lengths			Bond angles	
	Experimental	**Calculated**		**Experimental**	**Calculated**
Au1-Cl1	2.2517(10)	2.3900	Cl1-Au1-S1	174.87(4)	172.28
Au1-S1	2.2649(10)	2.4654	C8-S1-Au1	104.39(12)	101.39
S1-C8	1.701(4)	1.7808	C8-N1-C7	128.7(3)	127.66
O1-C7	1.213(4)	1.2650	C8-N2-C9	126.5 (3)	125.36
N1-C8	1.355(4)	1.3887	C2-C1-C6	119.0 (4)	119.54
N1-C7	1.378(5)	1.4059	C2-C1-C7	117.8 (4)	116.77
N2-C8	1.313(4)	1.3396	O1-C7-C1	123.3 (3)	122.98
N2-C9	1.444(4)	1.4527	O1-C7-N1	120.8	120.20
C1-C7	1.480(5)	1.4801	C7-C1-C6	123.2 (3)	123.69
C1-C2	1.375(5)	1.4158	C2-C3-C4	119.8	119.98
C1-C6	1.380(5)	1.4178	N2-C8-S1	122.4(3)	121.76
C2-C3	1.379(6)	1.4018	N1-C8-S1	119.9(3)	119.9
C3-C4	1.355(7)	1.4101			
C4-C5	1.370(7)	1.4085			

9.3. Frontier Molecular Analysis and Global parameters

The energy of LUMO and HOMO molecular orbitals and other related parameters are of prime interest for chemists, physicists and material scientists. Energies of frontiers orbitals decide whether the molecule is soft or hard. The frontier orbitals also predict the most reactive position in π-electron system and energy gap between HOMO and LUMO are also used for interpreting the chemical stability of a molecule. The HOMO has the ability to donate electrons, while LUMO accepts electrons and these two levels are very important for coordination chemists. These orbitals predict the coordination behavior of an organic molecule to act as ligand and/or to accept electrons from the metal ion during back bonding. The position of HOMO and LUMO in a molecule also determine the softness or hardness of the ligand. The ionization potential is the energy of HOMO, while the energy of LUMO is concerned with electron affinity. The energy difference between HOMO and LUMO is the band gap or energy gap and it corresponds to the kinetic stability and chemical reactivity of molecules. The energy gap calculated for ligand **L** is -0.144 eV and for complex **1** is -0.1.37 eV. Other global reactivity parameters are calculated using frontier orbital energies, given in Table 2. The frontier orbitals HOMO and LUMO of both ligand and complex **1** are given in Figure S4 and S5. The electronic cloud in HOMO is localized on C=S moiety in the ligand and in complex **1** these electrons are localized between metal ion and the C=S fragment. The LUMO of the ligand are localized on aromatic rings and S atom, while the same orbitals in metal complex are localized on aromatic rings.[42] These observations reveal that the ligand is considerably soft and has the ability to act as π-acceptor and to afford stable complexes with soft metals.

9.4. **Electrostatic potential analysis**

Molecular electrostatic potential (MEP) is generally used to explore molecular interactions. It is the potential experienced by a unit positive charge which surrounds the molecule due to the

distribution of electrons in the respective molecule. Electrostatic potential predicts the chemical reactivity of the molecule. The site of negative potential corresponds to be site of protonation and available for nucleophilic attack (electron rich), while the positive potential site is considered to be the site accessible for electrophilic attack [20, 21]. The 3D representation of complex **1** and the ligand **L** is shown in Figure S6 and S7, respectively, where the color scheme 'red' is a negative extreme and 'blue' is positive extreme. The order of increasing potential is red<orange<yellow<green<blue.

Table 2 Global reactivity parameters (eV) for ligand **L** and complex **1**

Compound	I	A	X	H	Σ	μ	Ω
Ligand	5.57	1.68	3.22	1.945	0.25	-3.625	3.36
Complex 1	6.53	2.83	4.68	1.85	0.27	-4.68	5.91

9.5. Cytotoxicity

Brine shrimp lethality bioassay is one of the rapid preliminary test for the biochemical activity of compounds. This test is based on the lethality potentials of any metal complex to brine shrimp nauplii. It is suggested that a test sample containing LC_{50} less than 1 mg/mL are considered most damaging to cells[25, 43, 44]. In present study the LC_{50} value of complexes **1-3** has been evaluated. Among all the three complexes the complex **1** exhibits maximum lethality after 24 h, which is quite promising and comparable to standard Doxorubicin (0.1 mg/mL) and may have anticancer effect on cancerous cells. The summarized data related to complex **1** and the standard (Doxorubicin) are represented in *Table 3*. Graphically the relationship of concentration *vs* mortality is represented in **Error! Reference source not found.** (for complex **1**).

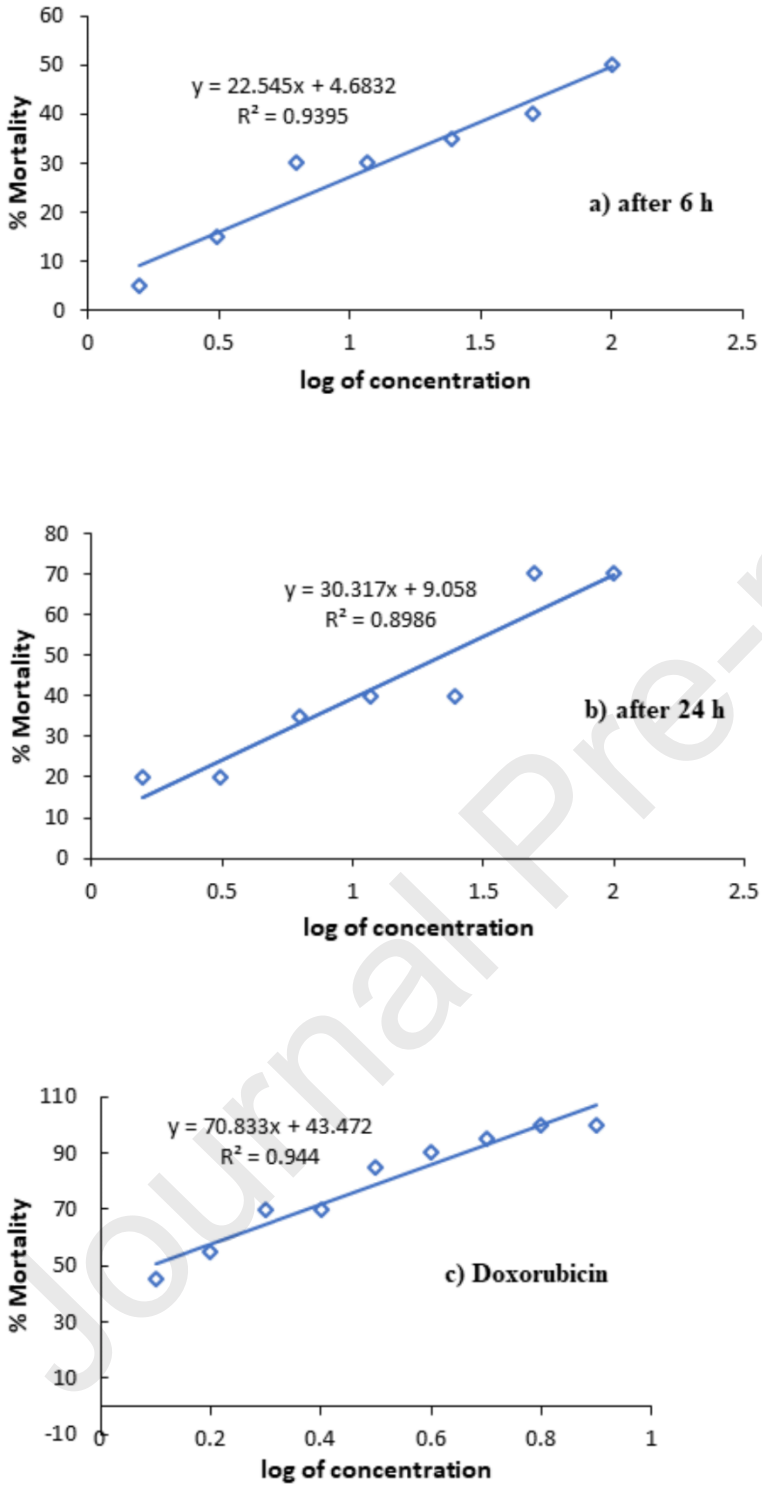

Figure 3 Brine shrimp lethality of a) complex **1** after 6 h, b) 24 h and c) Doxorubicin as positive control

Table 3 Summarized values of brine shrimp toxicity as LC_{50} value determined after 6 and 24 h.

Sample/control	**LC_{50} (mg/mL) after 6h**	**LC_{50} (mg/mL) after 24 h**
Complex **1**	2.06	1.35
Complex **2**	2.13	1.70
Complex **3**	2.41	1.87
Doxorubicin	0.1	0.1

9.6. Antibacterial Activities

The *in vitro* antibacterial activity of complexes **1-3** were tested against three gram negative bacterial strains namely *Bordetella bronchiseptica*, *Salmonella typhimurium* and *Enterobacter aerogenes*, the obtained results have been tabulated in

Table 4 and the same has been represented graphically in Figure 4. The activity of complexes **1-3** was compared with the available standard antibiotic, cefixime. Among complexes silver based complex was more potent with inhibition zones 17, 17 and 16 mm against *E. aerogenes*, *B. bronchiseptica* and *S. typhimurium,* respectively. Complex **1** exhibited relatively higher activity against *B. bronchiseptica* with inhibited zone of 18 mm (81.8%). The increased antibacterial activity of metal complex compared to free ligand can be explained as, ligand delocalizes its π electrons with metal ion and metal ion partially shares its positive charge with the ligand, which results decrease in polarity of the complex, consequently increase the lipophilicity of metal complex. This increased lipophilicity enhances penetration of metal complex to lipid membrane forming hydrogen bond with imine group by the active site which interfere enzyme activity, DNA damage and cell wall synthesis and finally may lead to cell apoptosis[45-47].

Table 4 Bacterial Inhibition data for complexes **1-3** against three selected strains.

Complex/Control	*Zone of Inhibition (mm)*		
	E. aerogenes ±*SE*	*B. bronchiseptica* ±*SE*	*S. typhimurium* ±*SE*
1	12±1.51	18±1.81	15±1.41
2	17±1.27	17±1.42	16.2±1.26
3	9.4±1.5	15±1.27	10.7±1.5
Cefixime	22±1.26	25±0.56	22±1.808

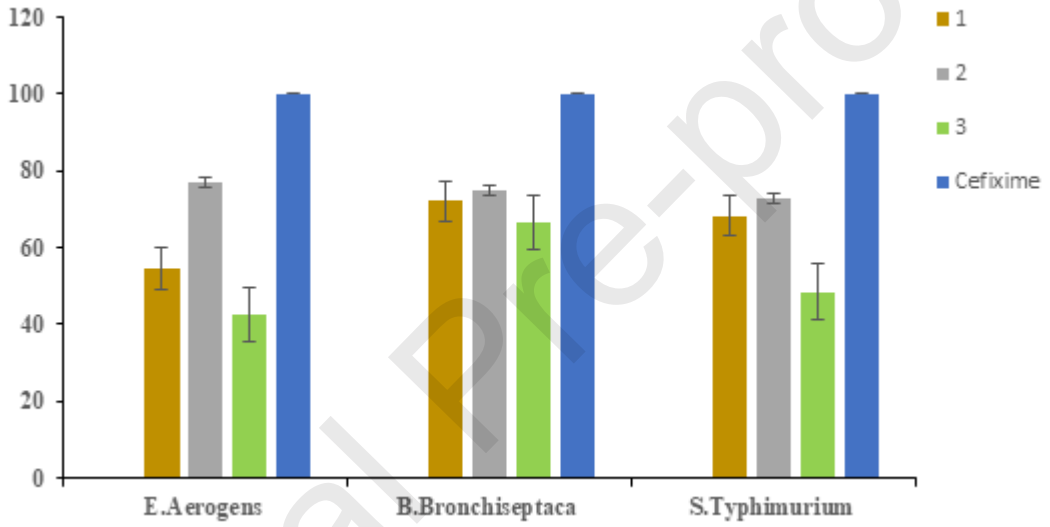

Figure 4 Graphical representation of zones of inhibition of complex **1-3** and the standard available drug, against three strains selected in this study.

9.7. Antifungal Activity

The *in vitro* antifungal activity of complexes **1-3** was determined against selected fungal *strains Aspergillus fumigatus, Fusarium solani and Mucor specie*. All the complexes are active against *Fusarium solani*, with inhibited zones of 17.5 (72.9%), 12.5 and 12 mm, respectively. The activity of complex **1**, was very poor against *Mucor specie* as compared to complexes **2** and **3.** The activity of complexes against *A. fumigatus* and *Mucor specie* was poor to moderate. On the basis of these results it can be concluded that these complexes cannot be used as better antifungal agents. The data obtained against the selected strains of fungi are summarized in *Table 5* and graphically

represented in Figure 5. The enhanced activity of coordinated ligand can be explained on the basis of chelation theory as discussed above for antibacterial activity [48-51].

Table 5 Fungal Inhibition data for complexes **1-3**:

Sample/Control	*Zone of Inhibition (mm)*		
	Aspergillus fumigatus±*SE*	*Fusarium solani*±*SE*	*Mucor* specie ±*SE*
Complex **1**	7.5±0.707	17.5±1.11	0
Complex **2**	7.0±0.5	12.5±0.8	7.7±0.85
Complex **3**	6.7±0.5	12±0.5	5.5±0.75
Terbinafine	24±1.21	21±1.11	22±1.61

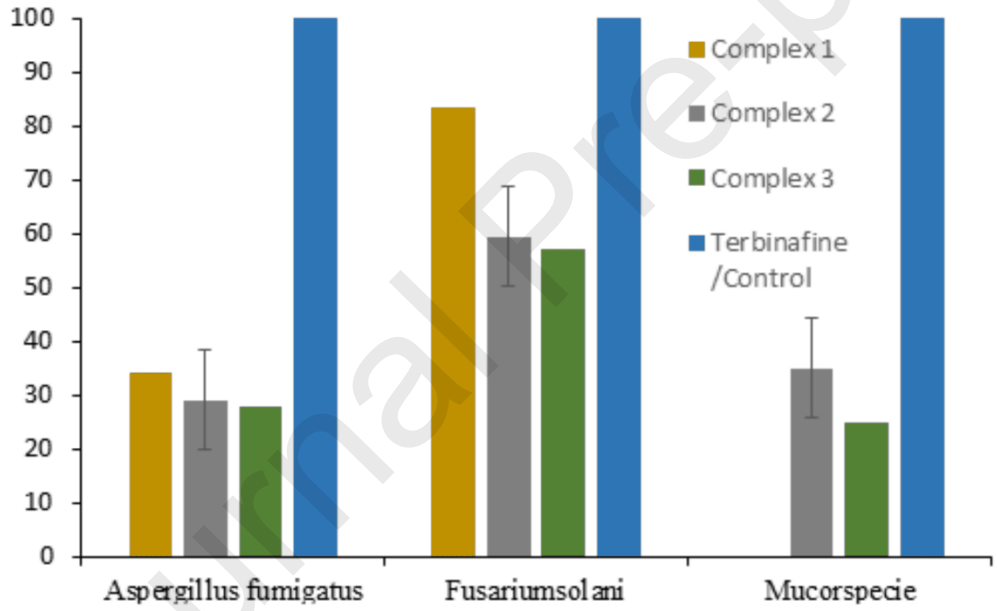

Figure 5 Graphical representation of fungal zones of inhibitions by complex **1-3**

9.8. DPPH Scavenging assay

DPPH is a stable free radical and its nature is affected by molecules capable of donating hydrogen atom or electron. Reactive Oxygen Species, ROS [52] are continuously produced in the form of free radicals in normal life processes of aerobic organisms. Over production of various free radicals in the body affect adversely the DNA bases, thus causing serious disorders. In human

beings the cancer, aging, chronic and oxidative stress can be associated with the production of free radicals [10, 53]. It is need of the day to have an efficient supplement as antioxidant in order to control the production of antioxidants or to neutralize them. Complexes **1-3** were investigated for their possible antioxidant activity against DPPH free radical. The complexes exhibited IC_{50} values 11.4, 35, 28 ppm with 69.87, 54.2 and 60.4%, respectively. The ascorbic acid was used as standard antioxidant during this study. Among complexes the activity of complex **1**, is far better than complex **2** and **3** and is very close to the activity recorded for the standard. The efficiency of complex **1**, is quite impressive in comparison to other metal based antioxidant [53, 54] but still it needs to be improved so that up to mark activity is achieved in order to make these reagents commercially viable.

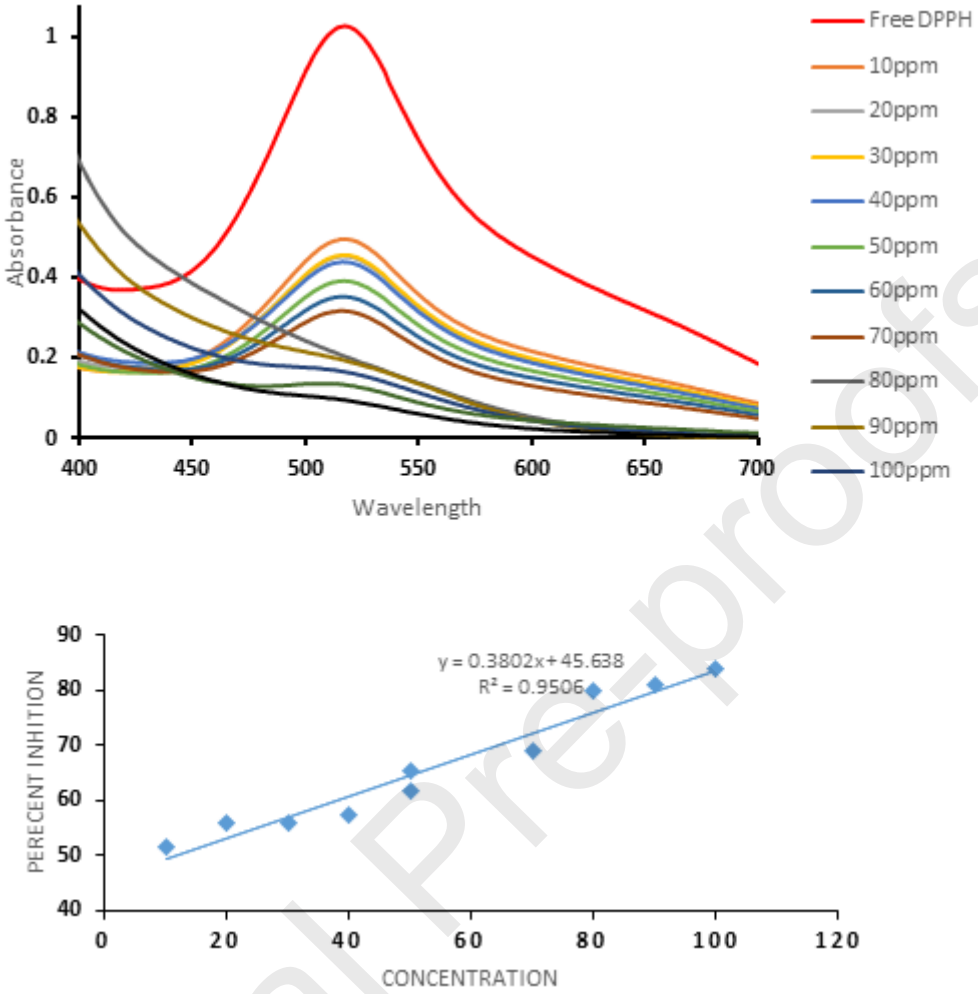

Figure 6 Free radical scavenging efficiency of complex **1**, which increases with increase in concentration of the complex in a dose dependent manner (upper), and plot indicating relationship between percent inhibition *vs* concentration of complex **1** used for calculating IC_{50} value.

9.9. DNA binding activities

9.9.1 UV- Visible studies

The interaction of complex **1-4** with DNA was studied by electronic absorption to determine the binding affinities of the target complexes. The binding mode of the complexes to DNA can be determined by the spectral changes (either increase or decrease in shift or intensity in wavelength) of complex upon the addition of DNA. The complex **2** did not show any change upon addition of DNA and hence was declared as inactive for DNA binding. Upon addition of different concentration of DNA to the solution of complex **1, 3** and **4** with constant concentration, a significant decrease in absorption peak was observed at 248, 247, 310 nm (hypochromic) with no detectable shift in wavelength, respectively. The gradual decrease in absorption shows interaction of complex with double strand of CT-DNA through intercalation, which was further confirmed through viscosity measurement (given in the following section). The binding constant K_b of complexes **1**, **3** and **4** were determined by plotting [DNA]/[ε_a-ε_f] vs [DNA] and was found to be 1.270×10^4, 1.646×10^4 and 2.178×104, respectively. The spectral change determined during experiments for complex **1**, **3** and **4** are given in Figure 7, Figure 8 and S8, respectively. The poor DNA bonding of efficiency of complex 4, supports the proposed structure of the complex where free sites are not accessible for interaction with DNA.

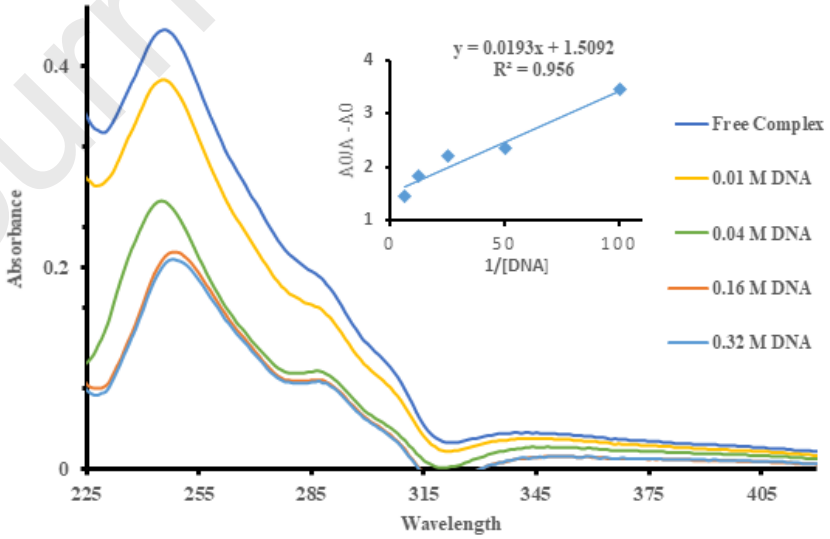

Figure 7 UV-visible spectra of complex **1**, indicating DNA binding

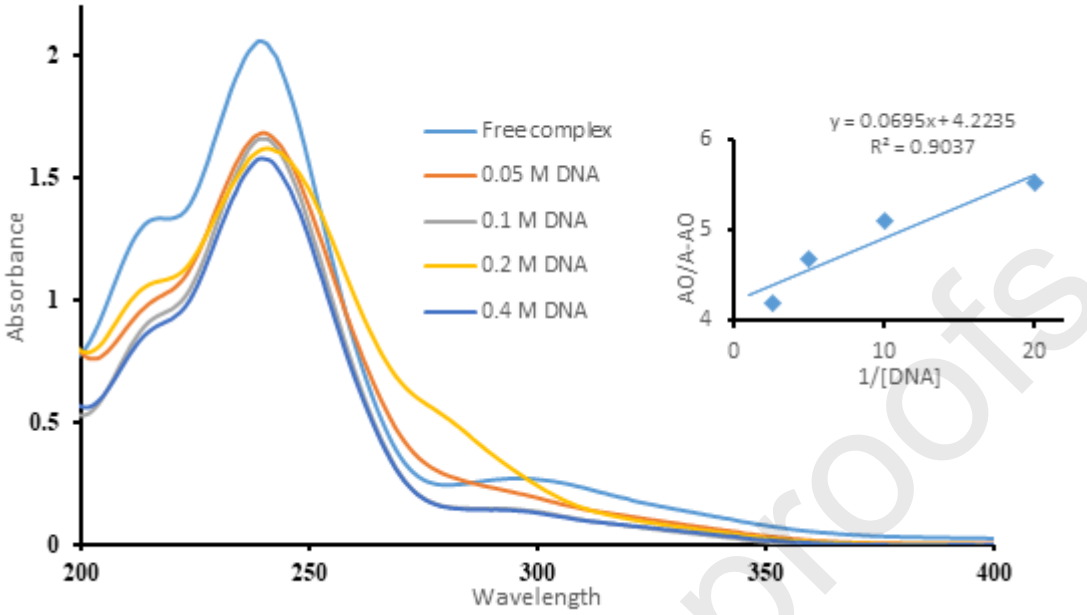

Figure 8 DNA binding studies through UV-visible spectroscopy of complex **3**

The absorbance for pure complex is maximum (**1**, **3** and **4**) and by addition of the DNA, the intensity abruptly/gradually changes. The decrease in absorbance is a function of interaction potentials of the respective complex with DNA. A comparison of complex **1**, **3** and **4** reveals that Au based linear complex **1** is more efficient than complex **3** and **4**.

9.9.2 Viscometry

Viscosity measurement provide critical information about the mode of interaction of a complex/compound with DNA and is considered to be the least ambiguous test. In classical intercalation mode of binding the complex lengthen the DNA helix by separating the base pair to accommodate the ligand. The increase in viscosity of DNA was observed in complex **1**, **3** and **4** suggesting classical intercalation mode of binding as shown collectively for both the complexes in Figure 9. The mode and intensity of interaction can thus be confirmed. The efficiency of complex **1** is expectedly prominent as compared with complex **3** and **4**, where in complex **3** very slight change in activity with increase in concentration was observed.

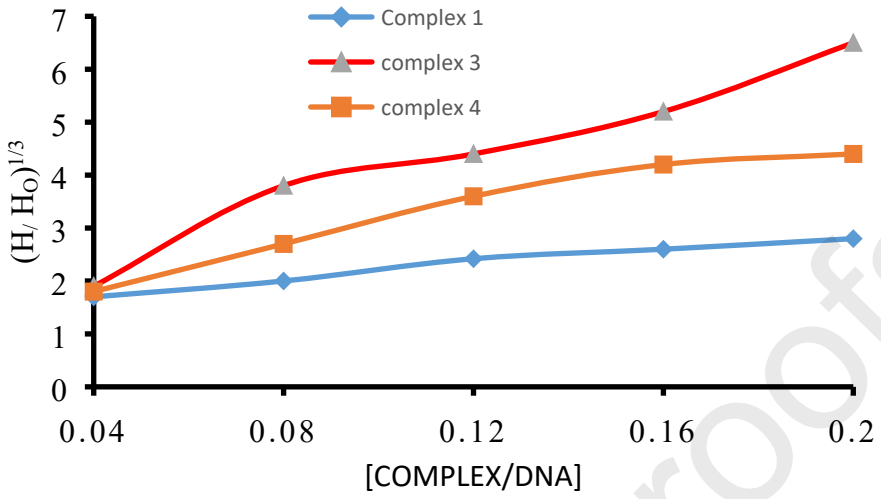

Figure 9 Plot of η/η°)1/3 vs [complex/DNA] of complex **1**, **3** and **4**.

10. Conclusion

Unsymmetrical thiourea (2,4,6-trimethylphenyl-3-benzoyl thiourea) as ligand is accessible in the laboratory and readily afford complexes of general formula MLX, where M = Au(I), Ag(I) and Cu(I), X = Cl^-, NO_3^- and I^- and $[ML_2]Cl_3$. Ligand was expected to give chelating complexes with S, O donor sites but the spectroscopic data reveal that Au affords mixture of two products. The products can be identified on the basis of their characteristic H-NMR chemical shifts and could be separated under microscope on the basis of their different crystalline shapes. Complexes **2** and **3** were pure compounds and formation of side product was not observed, however geometry around metal ion was different, linear around Au(I), Ag(I), trigonal around Cu(I) and square planar around Au(III). Complex **1** was isolated as crystalline material from the solid mixture and its structure was confirmed in solid state with the help of x-ray diffraction. All complexes exhibit promising antibacterial activities against *E. aerogenes*, *B. bronchiseptica* and *S. typhimurium*. Complex **1** exhibited higher activity (81.8%) against *B. bronchiseptica*, complex **2** was active against all three strains with zones of inhibition 17, 17 and 16 mm, respectively. Antifungal activity was in the same order and complex **1** (Au(I) based) was more active than Ag and Cu complexes. Antioxidant activities and DNA interaction were also studied and compounds were found to be of moderate efficiency. Experimental structural parameters of complex **1**, were compared with calculated data and a close agreement was found.

Conflict of Interest

Authors declare no interest of conflict

Acknowledgement

EK is thankful to Higher Education commission of Pakistan for financial assistance under NRPU project No. 7327.

Authors' Contribution

UAK performed experimental work required for his mandatory PhD degree, AB provided support for evaluating the samples for their biological efficacy in the Department of Chemistry, QAU, Islamabad, MNT collected diffraction data for single crystal of complex **1** and EK supervised the research work. The manuscript was jointly written by EK and UAK.

Appendix A. Supplementary data

CCDC No. 1979977 contains the supplementary crystallographic data for complex **1**. These data can be obtained free of charge via http://www.ccdc.cam.ac.uk/conts/retrieving.html, or from the Cambridge Crystallographic Data Centre, 12 Union Road, Cambridge CB2 1EZ, UK; fax: (+44) 1223-336-033; or e-mail: deposit@ccdc.cam.ac.uk.

References:

[1] S. Rafique, M. Idrees, A. Nasim, H. Akbar, A. Athar, Transition metal complexes as potential therapeutic agents, Biotechnology and Molecular Biology Reviews, 5 (2010) 38-45.

[2] A. Warra, Transition metal complexes and their application in drugs and cosmetics-a Review, J. Chem. Pharm. Res, 3 (2011) 951-958.

[3] C. Nieto-Oberhuber, M.P. Munoz, E. Bunuel, C. Nevado, D.J. Cardenas, A.M. Echavarren, Cationic gold (I) complexes: highly alkynophilic catalysts for the exo-and endo-cyclization of enynes, Angewandte Chemie International Edition, 43 (2004) 2402-2406.

[4] A.E. Pullen, S. Zeltner, R.-M. Olk, E. Hoyer, K.A. Abboud, J.R. Reynolds, Electrically conducting materials based on μ-tetrathiooxalato-bridged bimetallic Ni(II) anionic complexes, Inorganic Chemistry, 36 (1997) 4163-4171.

[5] B. Dominelli, J.D. Correia, F.E. Kühn, Medicinal applications of gold (I/III)-based complexes bearing N-heterocyclic carbene and phosphine ligands, Journal of Organometallic Chemistry, 866 (2018) 153-164.

[6] S. Wang, W. Shao, H. Li, C. Liu, K. Wang, J. Zhang, Synthesis, characterization and cytotoxicity of the gold (III) complexes of 4, 5-dihydropyrazole-1-carbothioamide derivatives, European Journal of Medicinal Chemistry, 46 (2011) 1914-1918.

[7] J.-J. Wei, J.-J. Xiao, J.-W. Yu, X.-Y. Yi, S. Liu, G.-Y. Liu, Synthesis and structural characterization of silver (I) and gold (I) complexes of N, N′-diisobutyloxycarbonyl-N ″, N‴-(1, 3-propylene)-bisthiourea, Polyhedron, 137 (2017) 176-181.

[8] A. Colak, Ü. Terzi, M. Col, Ş.A. Karaoglu, S. Karaböcek, A. Küçükdumlu, F.A. Ayaz, DNA binding, antioxidant and antimicrobial activities of homo-and heteronuclear copper (II) and nickel (II) complexes with new oxime-type ligands, European Journal of Medicinal Chemistry, 45 (2010) 5169-5175.

[9] D. Li, Y. Sun, S. Liu, Z. Hua, Synthesis, characterization and crystal structure of copper (I) tetra (phenyl thiourea) chloride, Journal of Coordination Chemistry, 59 (2006) 403-408.

[10] Z.-C. Liu, B.-D. Wang, B. Li, Q. Wang, Z.-Y. Yang, T.-R. Li, Y. Li, Crystal structures, DNA-binding and cytotoxic activities studies of Cu (II) complexes with 2-oxo-quinoline-3-carbaldehyde Schiff-bases, European Journal of Medicinal Chemistry, 45 (2010) 5353-5361.

[11] A.A. Altaf, A. Shahzad, Z. Gul, S.A. Khan, A. Badshah, M.N. Tahir, Z.I. Zafar, E. Khan, Synthesis, crystal structure, and DFT calculations of 1, 3-diisobutyl thiourea, Journal of Chemistry, 2015 (2015), Article ID 913435.

[12] D. Wang, S.Y. Wu, H.P. Li, Y. Yang, H.W. Roesky, Synthesis and Characterization of Copper Complexes with the N-(2, 6-Diisopropylphenyl)-N′-acylthiourea Ligands, European Journal of Inorganic Chemistry, 2017 (2017) 1406-1413.

[13] G.M. Sheldrick, A short history of SHELX, Acta Crystallographica Section A: Foundations of Crystallography, 64 (2008) 112-122.

[14] A. Hossain, T. Mandal, M. Mitra, P. Manna, A. Bauzá, A. Frontera, S.K. Seth, S. Mukhopadhyay, Exploring 3D non-interpenetrated metal–organic framework with malonate-bridged Co (II) coordination polymer: structural elucidation and theoretical study, Phase Transitions, 90 (2017) 1193-1204.

[15] A. Bruker, Inc.(2000–2012), Apex2 (Version 2012.2-0), SAINT+(Version 8.18 c), SADABS (Version 2008/1), and SHELXTL (Version 6.14). Bruker Advanced X-ray Solutions, Madison, Wisconsin, USA, (2012).

[16] A.L. Spek, Structure validation in chemical crystallography, Acta Crystallographica Section D: Biological Crystallography, 65 (2009) 148-155.

[17] K. SAYIN, D. KARAKAŞ, Method and basis set investigation for trans-platinum (II) oxime complex, Cumhuriyet Üniversitesi Fen-Edebiyat Fakültesi Fen Bilimleri Dergisi, 36 (2015) 1-10.

[18] K. Hollmann, A. Oppermann, M. Witte, S. Li, M. Amen, U. Flörke, H. Egold, G. Henkel, S. Herres-Pawlis, Copper (I) complexes with thiourea derivatives as ligands: revealing secrets of their bonding Scheme, European Journal of Inorganic Chemistry, 2017 (2017) 1266-1279.

[19] R. Kang, H. Chen, S. Shaik, J. Yao, Assessment of theoretical methods for complexes of gold (I) and gold (III) with unsaturated aliphatic hydrocarbon: Which density functional should we choose?, Journal of Chemical Theory and Computation, 7 (2011) 4002-4011.

[20] P. Itte, M. Amshumali, M. Pasha, Molecular modeling, geometry optimization and characterization of bimetallic complexes derived from s-indacene, Universal Journal of Chemistry, 5 (2017) 48-57.

[21] M. Drissi, N. Benhalima, Y. Megrouss, R. Rachida, A. Chouaih, F. Hamzaoui, Theoretical and experimental electrostatic potential around the m-nitrophenol molecule, Molecules, 20 (2015) 4042-4054.

[22] E. Khan, M. Khalid, Z. Gul, A. Shahzad, M.N. Tahir, H.M. Asif, S. Asim, A.A.C. Braga, Molecular structure of 1, 4-bis (substituted-carbonyl) benzene: A combined experimental and theoretical approach, Journal of Molecular Structure, (2019) 127633.

[23] M.N. Patel, B.S. Bhatt, P.A. Dosi, DNA binding, cytotoxicity and DNA cleavage promoted by gold (III) complexes, Inorganic Chemistry Communications, 29 (2013) 190-193.

[24] S. Naz, S. Tabassum, N. Freitas Fernandes, M. Mujahid, M. Zia, E.J. Carcache de Blanco, Anticancer and antibacterial potential of Rhus punjabensis and CuO nanoparticles, Natural Product Research, (2018) 1-6.

[25] A.R.M. Syahmi, S. Vijayarathna, S. Sasidharan, L.Y. Latha, Y.P. Kwan, Y.L. Lau, L.N. Shin, Y. Chen, Acute oral toxicity and brine shrimp lethality of Elaeis guineensis Jacq.,(oil palm leaf) methanol extract, Molecules, 15 (2010) 8111-8121.

[26] S. Tabassum, M. Ahmed, B. Mirza, M. Naeem, M. Zia, Z.K. Shanwari, G.M. Khan, Appraisal of phytochemical and in vitro biological attributes of an unexplored folklore: Rhus Punjabensis Stewart, BMC Complementary and Alternative Medicine, 17 (2017) 146.

[27] R.A. Hussain, A. Badshah, M.N. Tahir, T.u. Hassan, A. Bano, Synthesis, chemical characterization, DNA binding, antioxidant, antibacterial, and antifungal activities of ferrocence incorporated selenoureas, Journal of Biochemical and Molecular Toxicology, 28 (2014) 60-68.

[28] M.K. Rauf, A. Talib, A. Badshah, S. Zaib, K. Shoaib, M. Shahid, U. Floerke, J. Iqbal, Solution-phase microwave assisted parallel synthesis of N, N'-disubstituted thioureas derived from benzoic acid: biological evaluation and molecular docking studies, European Journal of Medicinal Chemistry, 70 (2013) 487-496.

[29] A.A. Karagözler, B. Erdağ, Y.Ç. Emek, D.A. Uygun, Antioxidant activity and proline content of leaf extracts from Dorystoechas hastata, Food Chemistry, 111 (2008) 400-407.

[30] S.B. Bukhari, S. Memon, M. Mahroof-Tahir, M. Bhanger, Synthesis, characterization and antioxidant activity copper–quercetin complex, Spectrochimica Acta Part A: Molecular and Biomolecular Spectroscopy, 71 (2009) 1901-1906.

[31] E. Khan, U.A. Khan, A. Badshah, M.N. Tahir, A.A. Altaf, Supramolecular dithiocarbamatogold (III) complex a potential DNA binder and antioxidant agent, Journal of Molecular Structure, 1060 (2014) 150-155.

[32] N. Shahabadi, M. Pourfoulad, N.H. Moghadam, Experimental and computational studies on the effects of valganciclovir as an antiviral drug on calf thymus DNA, Nucleosides, Nucleotides and Nucleic Acids, 36 (2017) 31-48.

[33] A. Pal, B. Biswas, M. Mitra, S. Rajalakshmi, C.S. Purohit, S. Hazra, G.S. Kumar, B.U. Nair, R. Ghosh, DNA binding and cleavage activity by a mononuclear iron (II) Schiff base complex: Synthesis and structural characterization, Journal of Chemical Sciences, 125 (2013) 1161-1168.

[34] J.K. Barton, J.M. Goldberg, C.V. Kumar, N.J. Turro, Binding modes and base specificity of tris (phenanthroline) ruthenium (II) enantiomers with nucleic acids: tuning the stereoselectivity, Journal of the American Chemical Society, 108 (1986) 2081-2088.

[35] A.H. Mageed, B.W. Skelton, M.V. Baker, Stable Au III complexes with four N-heterocyclic carbene groups can be prepared in high yield directly from KAuCl 4, Dalton Transactions, 46 (2017) 7844-7856.

[36] A.A. Isab, M. Fettouhi, S. Ahmad, L. Ouahab, Mixed ligand gold (I) complexes of phosphines and thiourea and X-ray structure of (thiourea-κS)(tricyclohexylphosphine) gold (I) chloride, Polyhedron, 22 (2003) 1349-1354.

[37] R.C. Luckay, F. Mebrahtu, C. Esterhuysen, K.R. Koch, Extraction and transport of gold (III) using some acyl (aroyl) thiourea ligands and a crystal structure of one of the complexes, Inorganic Chemistry Communications, 13 (2010) 468-470.

[38] K. Yan, C.-N. Lok, K. Bierla, C.-M. Che, Gold (I) complex of N, N′-disubstituted cyclic thiourea with in vitro and in vivo anticancer properties—potent tight-binding inhibition of thioredoxin reductase, Chemical Communications, 46 (2010) 7691-7693.

[39] L.C. Porter, J. Fackler, J. Costamagna, R. Schmidt, Structure of bis (thiourea) gold (I) bromide,[Au{SC(NH_2)$_2$}$_2$]Br, Acta Crystallographica Section C: Crystal Structure Communications, 48 (1992) 1751-1754.

[40] E. Khan, T. Ahmad, Z. Gul, F. Ullah, M.N. Tahir, A. Noor, Methyl-substituted 2-aminothiazole--based cobalt (II) and silver (I) complexes: synthesis, X-ray structures, and biological activities, Turkish Journal of Chemistry, 43 (2019) 857-868.

[41] A. Castiñeiras, N. Fernández-Hermida, R. Fernández-Rodríguez, I. García-Santos, Supramolecular Architecture in Gold(I) and Gold(III) 2-Pyridineformamide Thiosemicarbazone Complexes by Secondary Interactions: Synthesis, Structures, and Luminescent Properties, Crystal Growth & Design, 12 (2012) 1432-1442.

[42] S.I. Islam, S.B. Das, S. Chakrabarty, S. Hazra, A. Pandey, A. Patra, Synthesis, Characterization, and Biological Activity of Nickel(II) and Palladium(II) Complex with Pyrrolidine Dithiocarbamate (PDTC), Advances in Chemistry, 2016 (2016).

[43] M. Haque, M. Rahman, M.F. Hossen, M. Pervin, M. Kabir, K. Ferdaus, L. Bari, C. Zakaria, P. Hassan, M. Khalekuzzaman, In vitroantimicrobial and in vivo cytotoxic activity of some

ferrocene derivative bioactive metal complexes of first transition series, Pakistan Journal of Applied Science, 6 (2006) 988O992.

[44] A.F. Santos, D.F. Brotto, L.R. Favarin, N.A. Cabeza, G.R. Andrade, M. Batistote, A.A. Cavalheiro, A. Neves, D.C. Rodrigues, A. dos Anjos, Study of the antimicrobial activity of metal complexes and their ligands through bioassays applied to plant extracts, Revista Brasileira de Farmacognosia, 24 (2014) 309-315.

[45] P. Chetana, B. Srinatha, M. Somashekar, R. Policegoudra, Synthesis, spectroscopic characterisation, thermal analysis, DNA interaction and antibacterial activity of copper(I) complexes with N, N'-disubstituted thiourea, Journal of Molecular Structure, 1106 (2016) 352-365.

[46] N. Vamsikrishna, M.P. Kumar, G. Ramesh, N. Ganji, S. Daravath, DNA interactions and biocidal activity of metal complexes of benzothiazole Schiff bases: synthesis, characterization and validation, Journal of Chemical Sciences, 129 (2017) 609-622.

[47] C. Guran, M. Barboiu, P. Diaconescu, V. Iluc, M. Bojin, A. Scozzafava, C.T. Supuran, Synthesis and antifungal activity of metal complexes containing dichloro-tetramorpholino-cyclophosphazatriene, Metal-Based Drugs, 5 (1998) 287-294.

[48] M.A. Riswan Ahamed, R.S. Azarudeen, N.M. Kani, Antimicrobial applications of transition metal complexes of benzothiazole based terpolymer: synthesis, characterization, and effect on bacterial and fungal strains, Bioinorganic Chemistry and Applications, 2014 (2014).

[49] T.-R. Li, Z.-Y. Yang, B.-D. Wang, D.-D. Qin, Synthesis, characterization, antioxidant activity and DNA-binding studies of two rare earth (III) complexes with naringenin-2-hydroxy benzoyl hydrazone ligand, European Journal of Medicinal Chemistry, 43 (2008) 1688-1695.

[50] P.-x. Xi, Z.-h. Xu, X.-h. Liu, F.-j. Chen, Z.-z. Zeng, X.-w. Zhang, Y. Liu, Synthesis, characterization, antioxidant activity and DNA-binding studies of three rare earth (III) complexes with 1-(4-aminoantipyrine)-3-tosylurea ligand, Journal of fluorescence, 19 (2009) 63-72.

[51] W.H. Himratul-Aznita, N. Mohd-Al-Faisal, A. Fathilah, Determination of the percentage inhibition of diameter growth (PIDG) of Piper betle crude aqueous extract against oral Candida species, Journal of Medicinal Plants Research, 5 (2011) 878-884.

[52] S. Pellet-Rostaing, J.B. Regnouf-de-Vains, R. Lamartine, P. Meallier, S. Guittonneau, B. Fenet, Fluorescence Quenching of 2, 2'-Bithiazole-Containing Calix [4] arenes by Copper (I). Access to the corresponding [ML2],[ML], and [M2L] copper (I) complexes, Helvetica Chimica Acta, 80 (1997) 1229-1243.

[53] I.P. Ejidike, P.A. Ajibade, Synthesis, characterization, antioxidant, and antibacterial studies of some metal (II) complexes of tetradentate schiff base ligand:(4E)-4-[(2-(E)-[1-(2, 4-dihydroxyphenyl) ethylidene] aminoethyl) imino] pentan-2-one, Bioinorganic Chemistry and Applications, 2015 (2015).

[54] R. Datta, V. Ramya, Biologically Important Schiff Bases and Their Transition Metal Complexes, Mapana-Journal of Sciences, 11 (2012) 57-72.

Authors' Contribution

UAK performed experimental work for his mandatory PhD degree, AB provided support for evaluating the samples for their biological efficacy in the Department of Chemistry, QAU, Islamabad, MNT collected diffraction data for single crystal of complex **1** and EK supervised the research work. The manuscript was jointly written by EK and UAK.

Conflict of Interest

Authors declare no interest of conflict

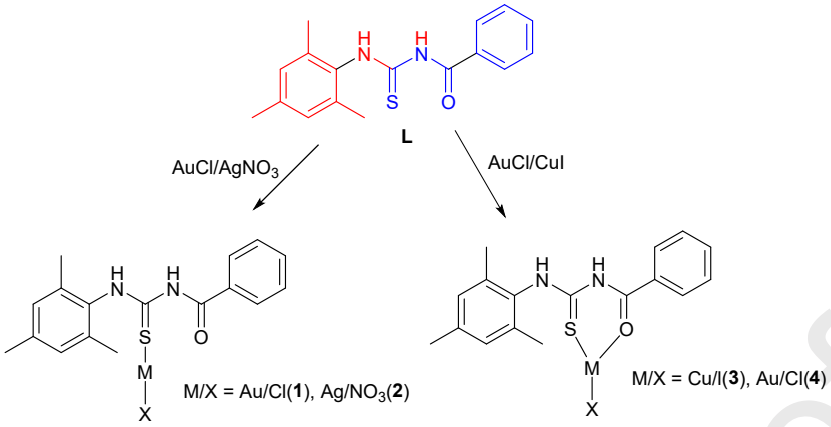

2,4,6-trimethylphenyl-3-benzoylthiourea and its coordination complexes were synthesized. All compounds were studied for their cytotoxicity, antibacterial, antifungal, antioxidant and DNA binding agents. The activities of complexes particularly Au-complex were promising. The structure of Au-complex was confirmed in solid state and the structural data was also calculated using DFT. The experimental and theoretical data were in close agreement.

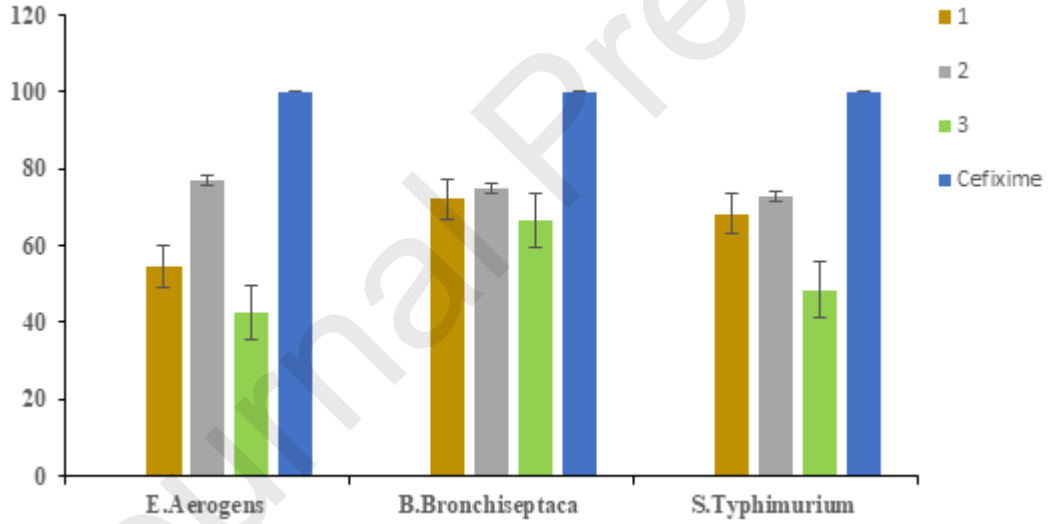

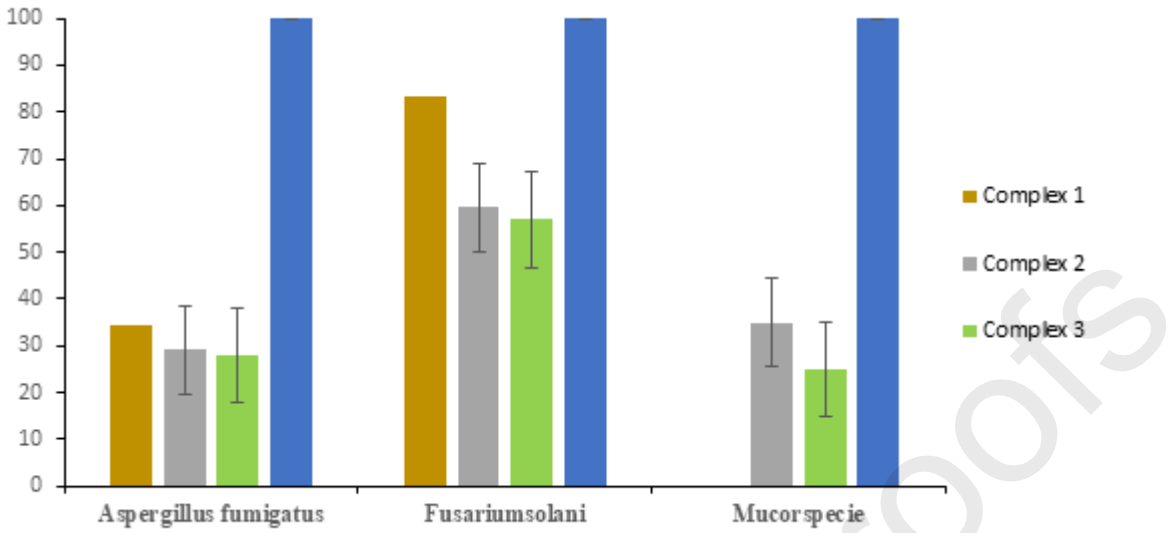

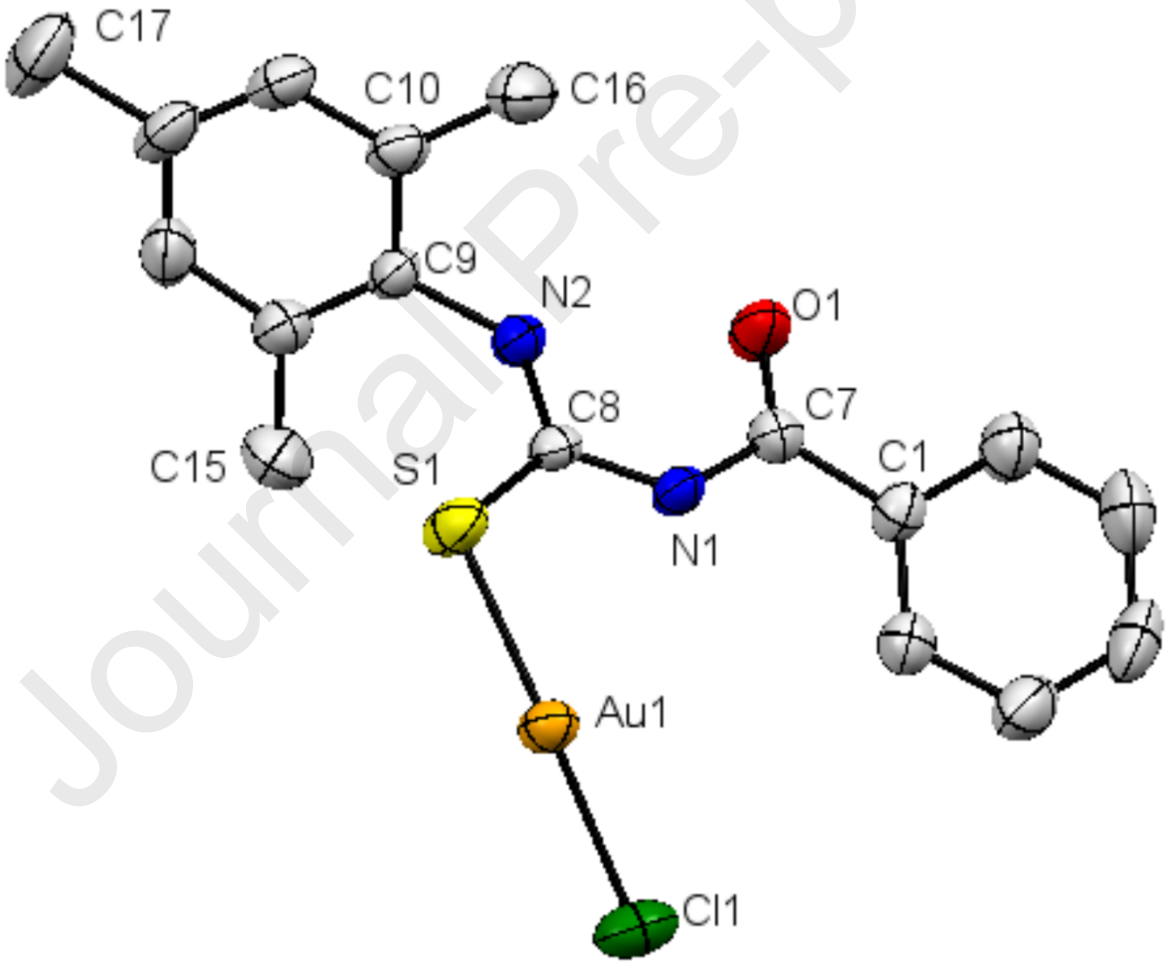

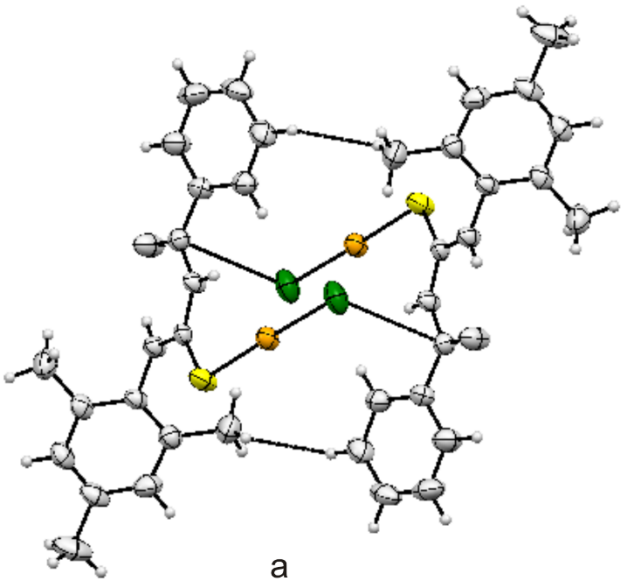

a

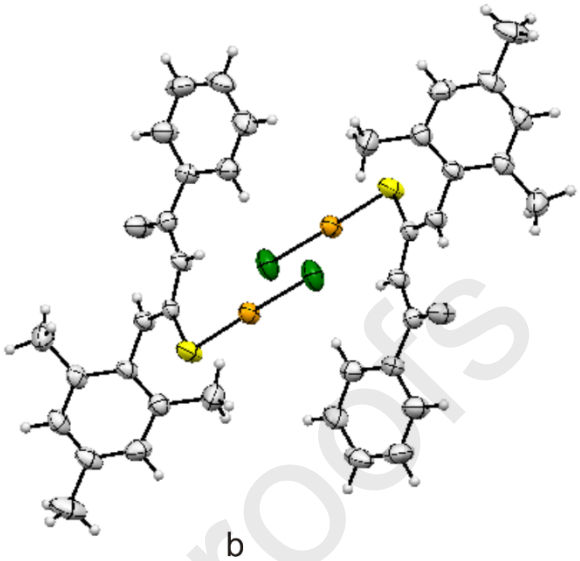

b

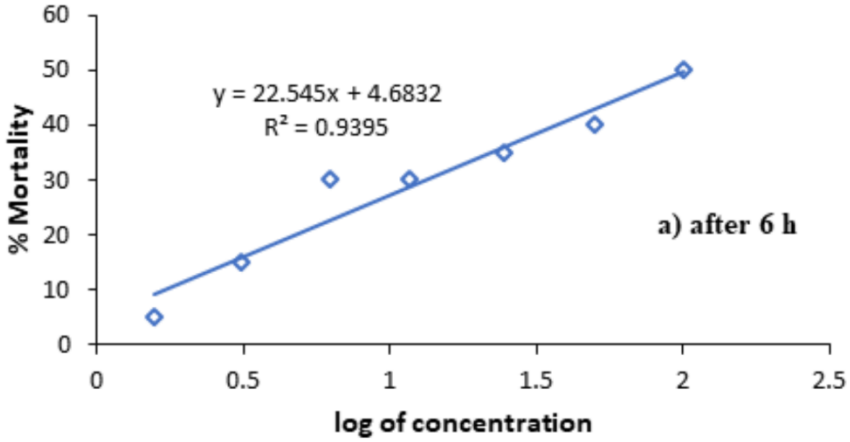

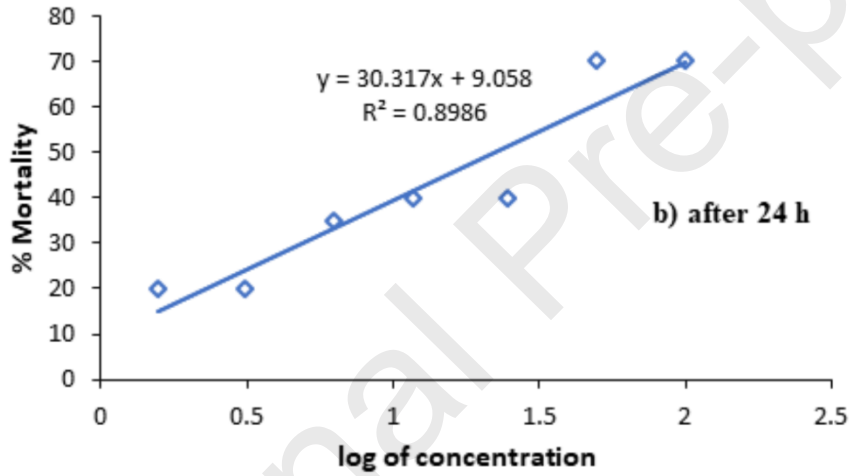

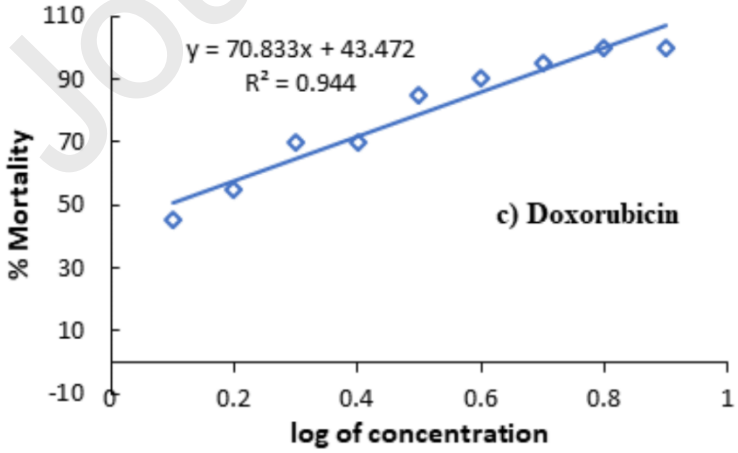

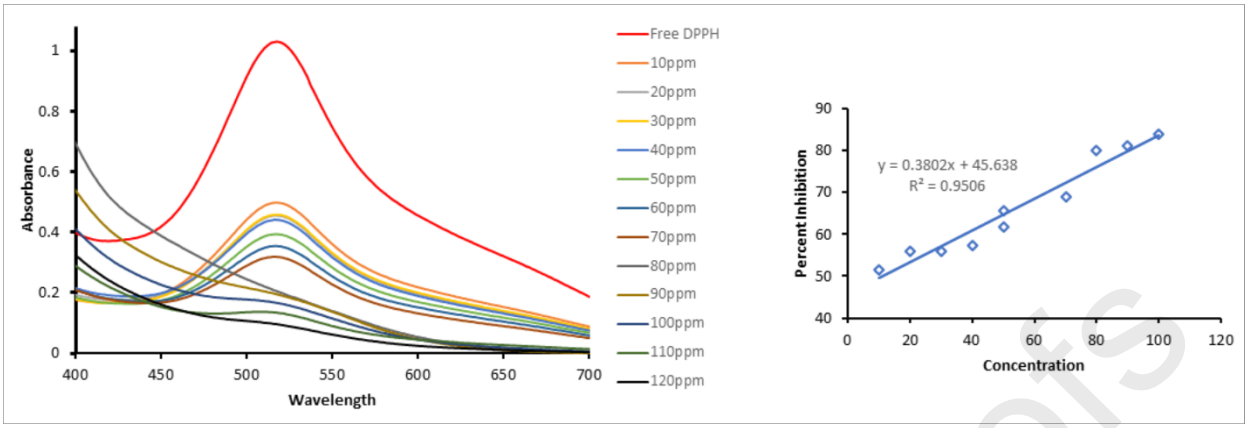

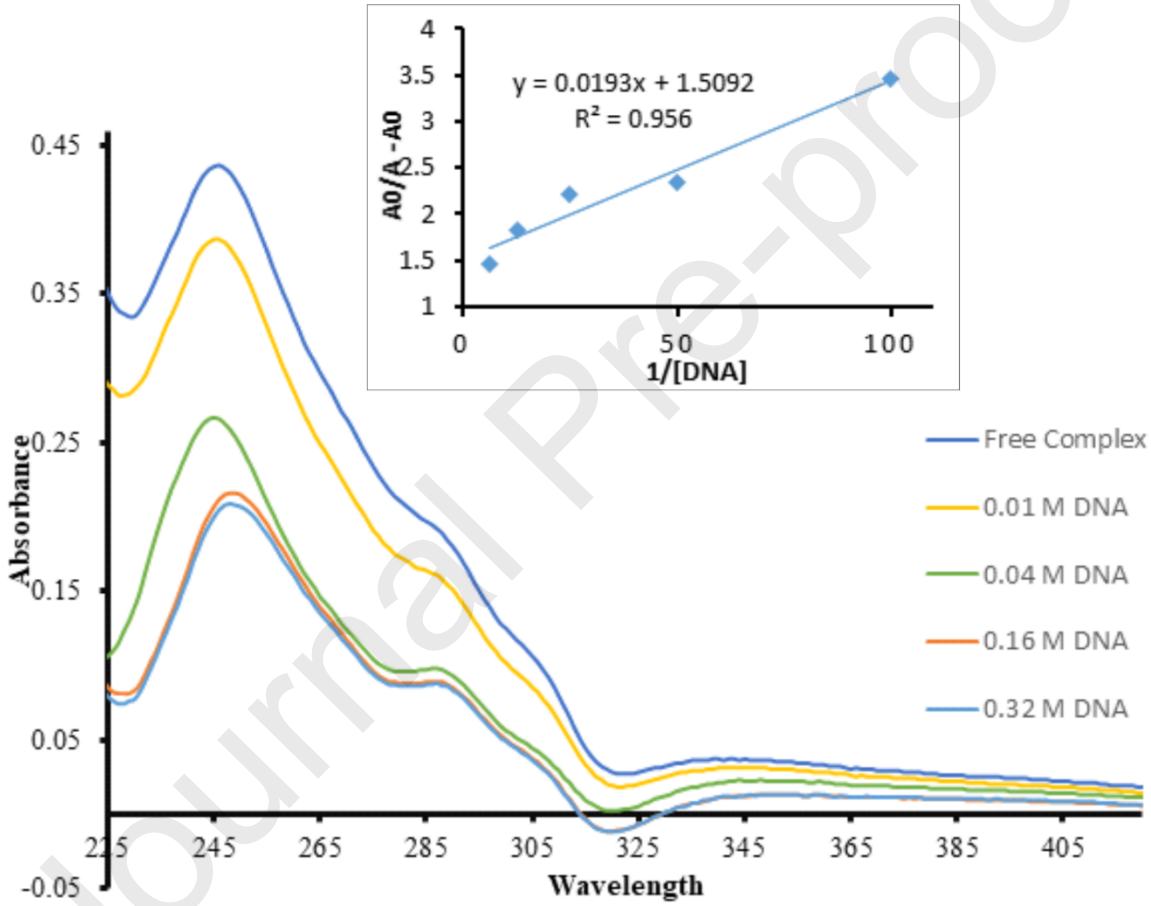

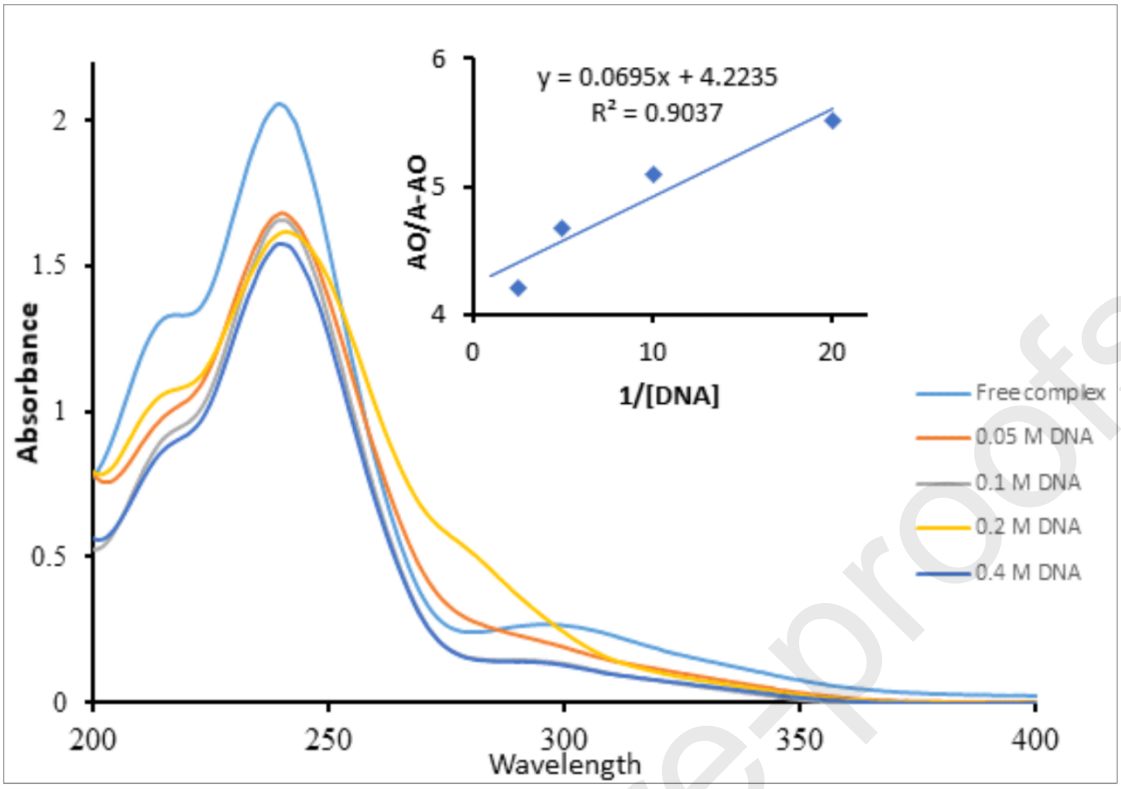

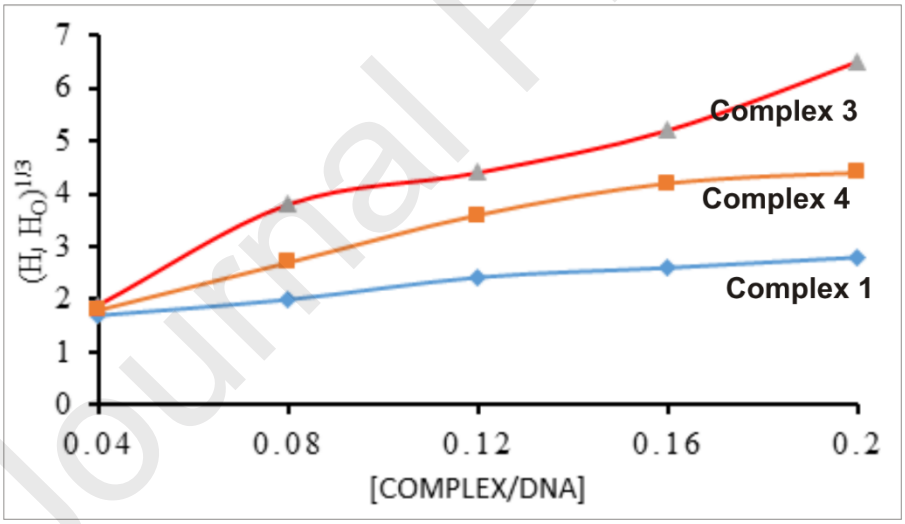

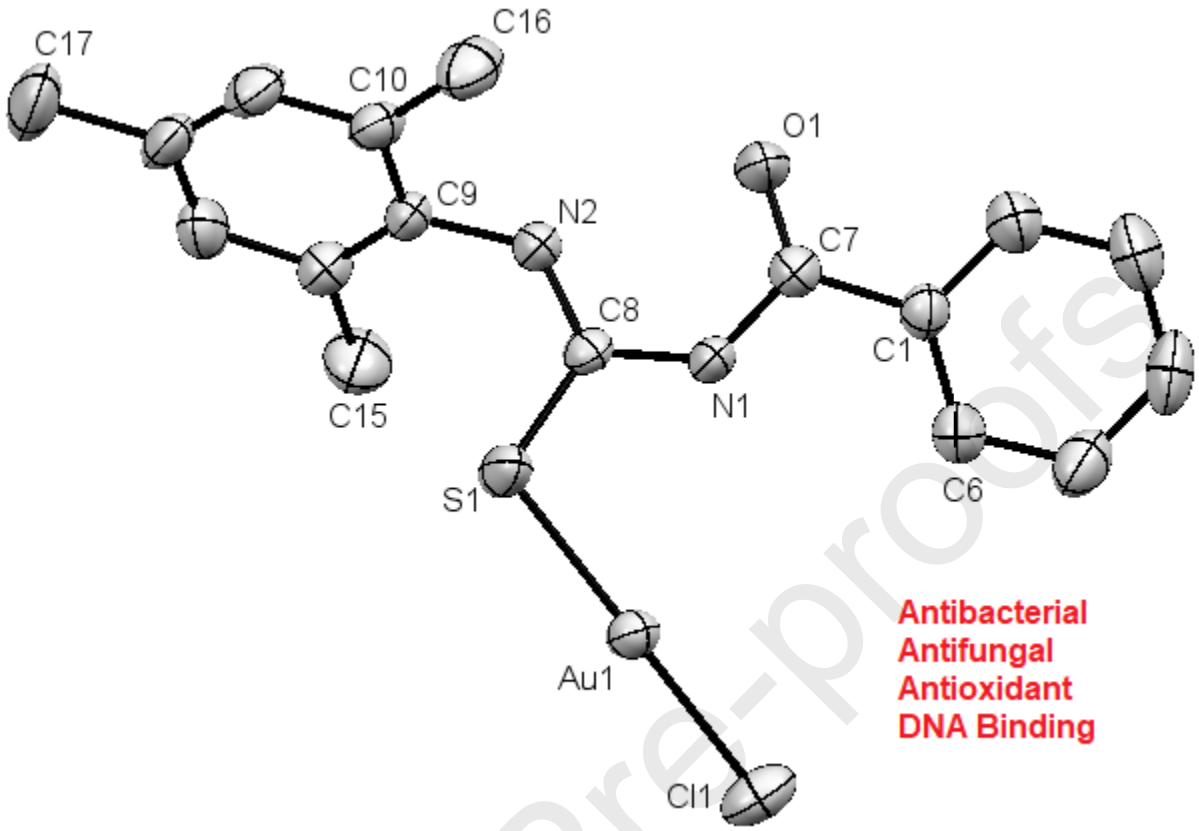

Antibacterial
Antifungal
Antioxidant
DNA Binding